National University of Lesotho

OPTIMIZATION OF THE CHOICE OF SOLAR MINIGRID ARCHITECTURE AND MANAGEMENT IN LESOTHO

MORUTI CLEMENT KAO

A dissertation submitted in partial fulfilment
of the requirements for the degree of

Master of Science in Sustainable Energy

Offered by the

Energy Research Centre
Faculty of Science & Technology

May 2020

Abstract

Installation and maintenance of the solar photovoltaic systems for power generation is highly discouraged by the high costs of storage units resulting from the traditional approach of sizing the systems. In order to reduce these costs, Solar PV systems sizing using a time-step approach is used in this study as opposed to traditional approach. Comparison of the traditional and time-step approaches used for sizing solar PV systems was performed and showed that time-step approach is the most cost-effective way of sizing the PV systems. The time-step approach is very important in this study since it addresses the country's lack of progress in mini-grid establishment regarding appropriate mini-grids architectural combinations versus costs best for Lesotho.

The primary aim of this research work was to develop a comprehensive computer-based model to be used for performance and optimization of mini-grid systems in order to reduce the system costs, operation costs as well as enhancing the systems reliability. This involved developing an approach to modelling hourly load profile in the absence of historical consumption data and finally determine the best mini-grid system architectural combination which should be used in Lesotho, based on considerations of reliability and cost of energy.

The current work successfully developed a simple computer-based program for optimally sizing, performance prediction and economic analysis of mini-grids systems. It shows how optimally sized solar mini-grid systems are determined by the model. The only data required to differentiate between mini-grid systems is the daily energy load as well as its hourly distribution and the desired supply reliability. The current work uses Sehong-hong mini-grid among sites identified by Sustainable Energy for All (SE4ALL) in Lesotho's mountainous districts and the objective function used for determining the cost effective solar mini-grid architectural combination best for Lesotho is the Levelized Cost of Energy (LCOE). The study also explores several diesel dispatch strategies on system performance and energy cost.

The study presents an optimised design and performance of solar mini-grid architectural configurations comprising solar PV array, solar inverter, battery bank, battery chargers as well as diesel generator. In this study, system component sizing is defined in terms of daily-energy-load related dimensionless variables, P/P_0 for PV array size, B_{cap}/L_{day} for battery size and $Q_{DG}/\bar{L}$ for diesel generator size. This allows generalization of the design for similar locations and similar hourly load profiles. Results of simulations using the study method show that the

most cost-effective configuration for mini-grid systems in Lesotho comprises a PV array, a battery and a diesel generator, and should operate at a high solar fraction. For 100% supply reliability, the optimum system comprises solar PV array size ($P/P_0 = 11.2$), battery bank size ($B_{cap}/L_{day} = 1.8$) and diesel generator size ($Q_{DG}/\bar{L} = 2.2$), operating at 83 % solar fraction and at LCOE of 0.62 *USD/kWh*. For 99% supply reliability, the optimum system has $P/P_0 = 3.9$, $B_{cap}/L_{day} = 0.292$ and ($Q_{DG}/\bar{L} = 2.2$), operating at 85% solar fraction and at LCOE of 0.30 *USD/kWh*. It is opined to go for 99% reliability ahead of 100% reliability as only a 1% increase in reliability results in 54% cost increase. The used dispatch strategy in this study for the diesel generator is charge cycling strategy.

Acknowledgements

My special thanks go to my supervisor, Engineer Tawanda Hove for providing me the wonderful opportunity and support to guide me in undertaking this MSc dissertation under his supervision, I feel really honoured. Dr Mpholo and the entire Energy Research Centre (ERC) in the National University of Lesotho, your guidance and information sharing were always key in making my job easier. Thank you for all the advice, ideas, moral support and patience in guiding me through this research work. The family members who were supporting me within thick and thin of this work, more especially Mrs. Mateetsa Kao, Mr. Mceno Tshehlana, Mr. Kao Tabampe, Mr. Elias Kao, Lindiwe Kao, Mrs. Malikotsi Kao, Mrs. Makhato Kao and more importantly my wife Mrs. Mabuyisiwe “Refiloe Manthelle Mpo” Kao. I am really honoured and thankful, may Almighty God be with you all.

Dedication

This work is dedicated to my two late souls, colleague and friend **DNA Ntjamang Daniel "Neymar" Alotsi**, a soldier who lost his life in our journey for MSc acquisition though was in different field. Man, it's my vivid hope that wherever you are, I made you proud. Rest in peace Tau. My late grandmother **Mamakoae Kao**, how I hope I was going to make you proud, but God's timing is always perfect, "Hamba Gahle Khomo".

Table of Contents

List of figures

List of tables

Acronyms and abbreviations

RETs	Renewable Energy Technologies
PV	Photovoltaic
SE4ALL	Sustainable Energy for All
HPS	Hybrid Power System
SSA	Sub-Saharan Africa
IEA	International Energy Agency
GHG	Green-House Gases
LCOE	Levelized Cost of Energy
MW	Mega-watt
GHI	Global Horizontal Irradiation
DC	Direct Current
AC	Alternating Current
NOCT	Nominal Operating Cell Temperature
SNL	Sandia National Laboratory
STC	Standard Test Conditions
DG	Diesel Generator
NCF	Net Cash Flow
IRR	Internal Rate of Return
NPV	Net Present Value
IC	Initial Costs
RC	Replacements Costs
O&M	Operation and Maintenance costs
SOC	Battery State of Charge
DOD	Maximum Depth of Discharge

Chapter 1

1. Introduction

This chapter entails a brief energy background globally, in African continent as well as in Lesotho in particular. An overview of the research problem and the research direction follows together with the rationale of the study, scope and outline of the structure and content of the entire dissertation report.

Globally, there is a recognizable and very significant technical advancements in power generation through renewable energy resources which are found to be progressively penetrating the global power generation. Nema et.al [1] highly appreciates and encourages these technical improvements since they are capable of delivering promising economic features, a significant major that makes renewable energy to be welcomed in the power systems sector. The initiative is also appreciated by Kumar et al.[2], seeing it as justifiably a great reinforcement for the rural electrification sector to overwrite experience learned from the previously failed rural electrification projects that experienced challenges such as incapability of supplying power at an affordable cost.

In order to effectively utilize the widespread of renewable energies, their quality and the quantity of that available renewable energy resources, it should be noted that renewable energy resources are highly location dependent. The major advantage of renewable resources is that they are environmentally friendly since they are emission free and unbound though they have a major disadvantage of being intermittent, particularly due to the uncontrollable weather and climatic conditions. Accurate and precise determination of available energy is hindered by this unpredictable weather behavior hence a combination of the renewable energy resource coupled with storage battery is determined to be very ideal to counter that intermittency associated with renewable energy sources to a considerable extent rather than utilizing a single energy source [1], [2].

Equipping these renewable energy resources with storage significantly improves supply reliability of these systems, which are thus referred to technically as Hybrid Power Systems (HPS). Apart from improvement of power supply reliability, the combination enables optimized utilization of local primary renewable energy resources [2]. Worldwide, the renewable energy hybrid systems have been deployed, particularly in the rural communities There are many hybrid systems deployed in many rural areas around the world. Solar hybrid systems are of two types, with the first type being those systems that constitute either electricity energy storage or multiple primary energy resources. Energy storage or the controlled energy source is appointed to counteract the intermittent behavior of renewable energies; thus, to maximize the availability of steady power supply to the loads. Therefore, hybrid systems provide an elegant solution to make rural electrification system to be self-supportive during surges and peak times.

1.1 Background

In sub-Saharan Africa (SSA), more than 620 million people are estimated to be lacking electricity according to the International Energy Agency report of 2014. Seven hundred and twenty million people are estimated to use inefficient and hazardous energy forms with 85% of them residing in the rural areas. This is thus having a negative impact on socio-economic well-being of those people in rural areas since electricity access plays a fundamental role in improving people's quality of life. Improvements in rural people's socio-economic conditions are hindered by lack of access to electricity as grid extension to those rural places with rugged terrain as well as low load factor was found to be extremely uneconomical[3]–[5].

Therefore, there is a need for development of the new methodologies accompanying new technologies to electrify rural people. Off-grid hybrid power systems composed of only renewable energy sources is highly recommended over the systems that comprises of complementary diesel generators due to economic and environmental rationale though initially there was a worldwide concern (socio-economic and environmental) particularly in developing countries about mini-grid energy production whether in the form at which it is provided can influence the social, economic, and the environmental conditions of the local communities for which the project is being implemented[6], [7].

According to Tenenbaum et. al [8], worldwide lack of access electricity is estimated at roughly 1 billion people even though the current progress in assuring energy access seems to be very slow to meet (Sustainable Development Goal 7) the target of universal electrification by 2030. The projections are that by 2030, roughly 674 million people will still remain un-electrified, with several reasons being assigned to that gap such as lack of financing. A total of $52 billion annually is needed in order to achieve universal access by 2030 though commitments currently taking place are estimated at less than half the required annual budget [8].

Apart from lack of financing, it is also discovered that electrification programs have traditionally focused entirely on national grid extension though that major seems to be mostly prohibitively expensive particularly in remote settlements and areas with low population densities, very challenging terrain mostly and low demand for electricity. The possible solution to this is to critically develop working electrification strategies or models capable of substituting grid extension. Practical substitution of expensive grid extension is found to be mini grids and off-grid systems [8].

Centralized power generation is a major electrification commitment that is seen as a significant contributor is the development of mini grids, which are estimated to have a potential of providing electricity access to more than 440 million people by 2030 who are currently having no access to energy as outlined by the International Energy Agency [9]. Solutions such as solar home systems and lanterns provide minor solutions because of their low wattage coverage for appliances such as lights and phone charging, hence mini-grids are identified as the missing link between grid-extension and individual, pico-scale solutions.

As stated by the International Energy Agency (IEA) report of 2011 [9], worldwide rural electrification through grid extension is very low with seventy percent of all rural areas lacking access to electricity. It is thus determined that in order to meet the SE4ALL goal of universal access by 2030, mini-grids are estimated to deliver forty percent of the new capacity. One of the challenges in Africa (Lesotho in particular) in quick establishment of mini-grids to counter the energy deficit experienced by the country is lack of knowledge about mini-grids technologies as well as best mini-grids architectural combination in Lesotho yielding required energy at lowest costs.

1.2 Problem Statement

The traditional approach used for sizing mini-grids cannot accurately analyse the performance of the mini-grid energy system since it uses a daily energy balance approach rather than a time-step approach. This approach does not take into account time-step variation of both the load and the renewable energy supply. It can therefore not tell if all hourly loads are satisfied (hourly reliability of the system). All the fore mentioned shortcomings lead to non-optimized system sizing. If under-sized, the system will have disappointing energy yields, and on the other end, if over-sized, it can translate into unnecessarily higher costs to consumers.

In Lesotho, Sustainable Energy for All (SE4ALL) have identified ten places which are regarded to be best for solar mini-grids establishment with reference to the available solar resource. The architectural structure that will be best for the country with maximum power output power at lowest costs remains the challenge since the country is still some miles backward in terms of mini-grids technology. Thus, a need has been identified for an appropriate method which can optimally size the stand-alone mini-grid system, by being able to determine the energy supply reliability as well as Levelised Cost of Energy. Hence this research will develop a computer-based program that can be used for performance prediction, economic analysis and therefore optimal sizing of mini-grid systems.

1.3 Problem Justification

When it comes to mini-grids power systems, high technology oriented countries have already done a massive and considerable amount of work. Contrarily, in developing African countries such as Lesotho, there has been relatively little work on the processes and mechanisms that facilitate more sustained operation of hybrid mini grids. Mini-grids development differs depending on different considered factors such as local conditions, capacity of the system, rural load profiles, system design in terms of architecture, implementation and operational budgets.

The first phase of Lesotho's mini-grids establishment brought in by SE4ALL still lack progress since proper knowledge in terms of mini-grids architectural combinations versus costs were not properly done since SE4ALL only passed a regulation that those mini-grids development should be purely renewable (no diesel generator). It is thus evident that SE4ALL only wanted to mitigate the greenhouse gases emissions (GHGs) without major view on the cost of energy at a prescribed reliability.

The knowledge from this study will thus address the strategic way of selecting the best solar mini-grid architectural combination aiming to come up with an optimized design that is viable, cost effective and most efficient. Also, this study intent to highly support and appreciate the mini-grid technology as it gains worldwide popularity as the possible solution to different countries' existing energy challenges. By virtue of proactive strategies as well as motivating greater utilization mini-grid technology for rural electrification, the study assures enhancement of existing knowledge on design and implementation of successful solar mini-grids.

1.4 Objectives

1.4.1 Main objective

To develop a comprehensive computer-based model to be used for performance and optimization of mini-grid systems in order to reduce the system costs, operation costs as well as enhancing the systems reliability.

To determine the best mini-grid system architectural combination which should be used in Lesotho, based on considerations of reliability and cost of energy.

1.4.2 Specific objectives

To develop an approach to modelling hourly load profile in the absence of historical consumption data.

To model the energy flows in a PV-battery-diesel generator system.

All the above mentioned objectives should be determined with the need to minimize the Levelised Cost of Energy.

1.5 Research Questions

- What is the best way to design an optimal mini-grid system?
- What is the best architecture of mini-grid systems appropriate for Lesotho?
- Which mini-grid architectural combination is best economic choice?
- What is the impact or improvement this study has when compared to traditional approach of sizing mini-grid systems?

1.6 Research Scope

The scope of this research is to technically design a program (excel based) that can be used to determine the best solar mini-grid architectural combination with lowest Levelised cost of energy. A place called Sehong-hong has been used as the case study in this current study particularly because it is one of the selected places by SE4ALL for mini-grids development. This study aims at analyzing, modelling and determining the optimal architectural configuration that will be ideal for mini-grid development in Lesotho.

1.7 Dissertation Organization

These current research work is categorized into five chapters, with chapter one giving out the general background to the study; problem statement, the objectives of the study and the significance of the study. Chapter two entails the review of literature, dealing with different modellings such as radiation modelling, cell temperature as well as PV output power modelling. Also, mini-grid technology in detail is demonstrated in this chapter.

Chapter three illustrates the methodology, which include data collection and validation, design analysis procedures, calculations and further optimizations. Results and discussions are in chapter 4 and the last chapter (chapter 5) provides the final reached conclusions by the study.

Chapter 2

2. Literature Review

As stated by Gupta et al. [10], potential development of a solar mini-grid for electricity generation depends on availability of various parameters such as temporal, local, global and spatially variable conditions. The discussed literature review in this study include the factors that influence PV potential including incoming solar radiation, radiation modelling, effects of panel efficiency as well as output power estimation.

The country's energy overview is discussed in section 2.1, sections 2.2-2.5 discuss mini-grids, their different types as well as different solar mini-grid architectural structures. Sections 2.6-2.10 discuss solar energy resource, solar radiation on tilted planes and existing methods for modeling incoming solar radiation and some conducted studies that were comparing performance of different models. Section 2.11 and 2.12 deals with cell temperature estimation and models used to estimate it. Lastly, the chapter concludes by the economic analysis of a solar PV system discussed in Section 2.13.

2.1 Lesotho energy overview

The Lesotho Electrification Master Plan report [11] states that the country has abundant solar, wind, and hydropower resources. This was further elaborated in “Scaling-Up Renewable Energy Program Investment Plan for Lesotho” (2017) [12] that solar potential in Lesotho is 188 MW, approximated 14 000 MW hydropower potential which include the 22 mini-hydropower sites as well as 2 077 MW wind potential. Different economic, technical and environmental plays a major role in determining the best renewable energy technology choice suitable for the country. The Global Horizontal Irradiation (GHI) in Lesotho ranges between 1 700 and 2100 kWh/m^2 annually, and it varies according to different places.

The country has daily 10.5 daylight hours as well as 13.5 daily daylight hours in winter and summer respectively. The major advantage of solar energy in Lesotho is that there is plenty of solar resource with more than 300 days of sunshine and that makes PV technology good enough for the country considering also its competitiveness, technological & market maturity. The only exception is during rainy days, as the overall performance of the PV system will drop. The average insolation ranges from 5.25-5.53 $kWh/m^2/day$ and this clearly indicates a real potential in solar renewable energy in increasing their contribution in the overall energy mix [11], [13].

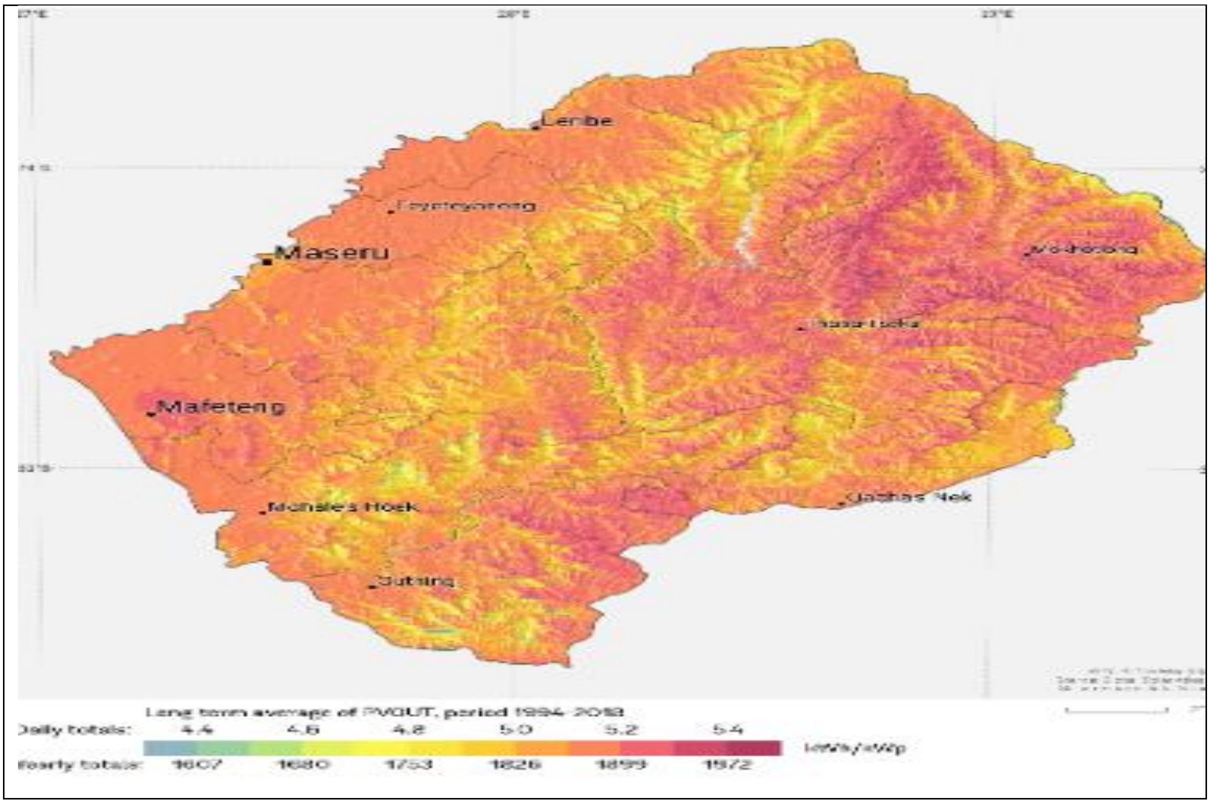

Figure 1: Solar resource map of Lesotho illustrating PV output potential [14]

The renewable energy development in Lesotho received a bigger support from the government with the development partners by the government's side. The country's major power comes from a 72 MW 'Muela hydropower plant but there is also a 281 kW installed solar photovoltaic plant situated at Moshoeshoe I International Airport as well as multiple small hydropower plants in the country [12].

Lesotho through its government suggests utilization of these abundance of solar energy it has, as well as wind/hydro resources, where available, so as to meet rural communities' energy needs, with reference to the context of the United Nations Sustainable Energy for All Initiative. The three objectives of the Sustainable Energy for All Initiative are to ensure universal access to modern energy services, double the rate of improvement in energy efficiency and double the share of renewable energy in the global energy mix by 2030. As a result, there is a determined perception among decision makers' desire to shift towards more decentralized, sustainable and modern forms of energy for the scattered rural areas to enable them to cook, light and heat their communities particularly during the winter months [12].

2.2 Mini-grids

Mini-grid is the fastest growing technology in recent years in the distribution part of renewable energy worldwide. This lead to several governments of most countries accepting it as a major alternative to grid-based electrification having enough capacity to provide remote areas with much needed clean electricity services access not in possession to reach the national grid in order to enhance their socio-economic development. This technological development was also found to be idea as it acts as an initiative to support underdeveloped rural energy problems as well as issues associated with climate change[15]–[17].

Mini-grids are systems that entail small-scale electricity generation (up to 10 MW) serving a limited number of consumers. Mini-grids evolve via a distribution grid or operate in isolation from the national transmission networks as demonstrated in figures 3 and 4 respectively.

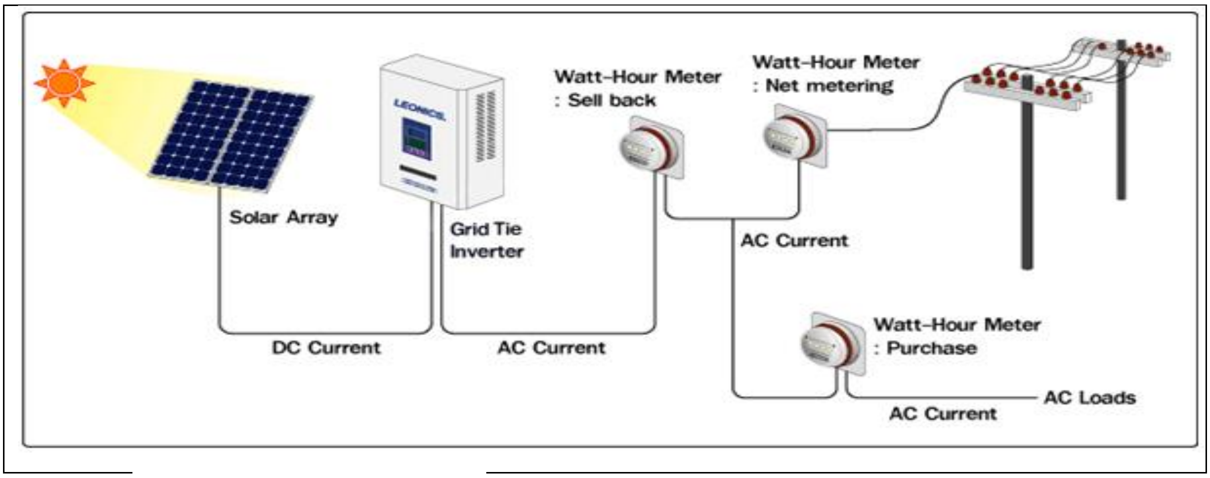

Figure 2: A grid-tied solar PV system[18]

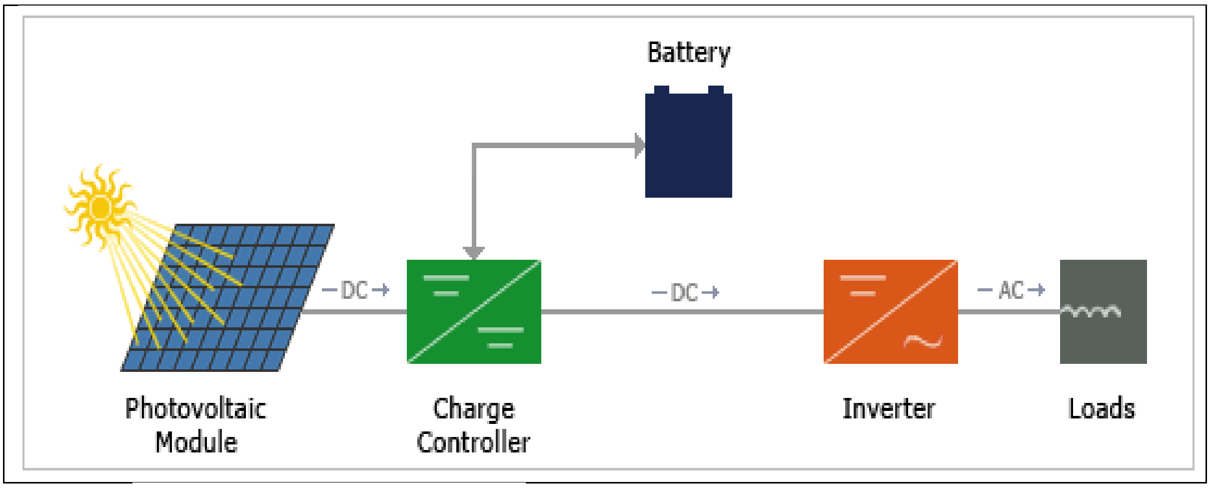

Figure 3: A stand-alone solar PV system[19]

Mini-grids originally operated only by diesel generators but currently their reliability and competitiveness can be enhanced by equipping them with renewable energy and storage systems. Sometimes, hybridization of all mini-grids is restricted by limited resources. Renewable energy technologies' price decline and technical progress have made rural electrification which was once an unprofitable business, an accelerating one now around the world [20], [21].

Naturally, mini-grids are purely different from the known single consumer systems like solar cell panel that is used for supplying electricity in a single house, in which various customers are not interconnected. Considering the fact that mini-grids are composed of different sizes or capacities, they service a cluster of up to 500 households, street lighting, schools, telecommunication systems powered by photovoltaic which has a total energy demand between 20 kWh and lower per day, small business, and refrigeration [22], [23] As outlined in Kenya's electricity report [24] about the role of renewable energy mini-grids, they are the super promising power configurations that are competent to enhance energy access to a very bigger portion of the 1.2 billion habitants lacking electricity access in developing countries, Africa in particular comprising a number of such people because the anticipated population growth is exacerbating that situation.

2.2.1 Components of PV mini-grid system

Photovoltaic mini-grid systems consist of the following fundamental components:

PV Array

A connection of several solar modules is referred to as PV array. A single solar module consists of a number of solar cells (composed of silicon (Si)) which are either connected in series or parallel.

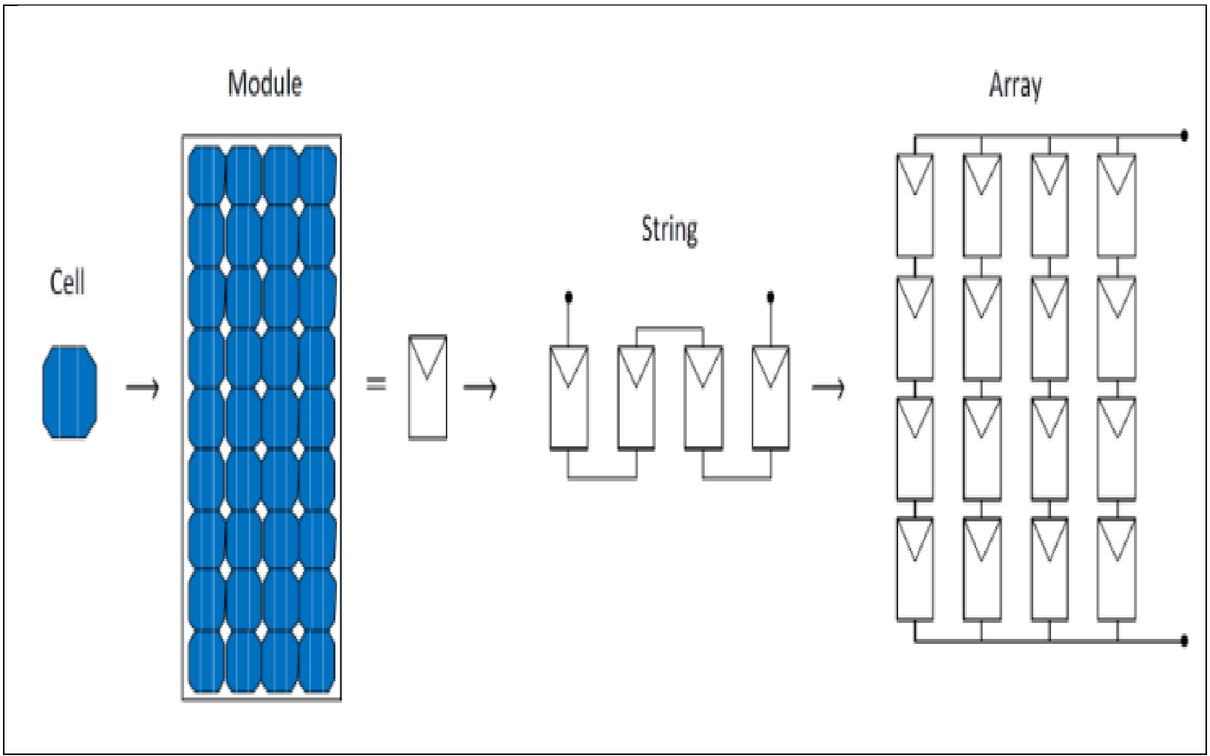

Figure 4: Solar PV array configuration [25]

The solar cell's performance depends on the variation of the output voltage as well as the current as illustrated in figure 4. The produced power by the solar cell is determined to be the product of the output current and voltage under operating characteristics, with the maximum power of the PV module brought about the product of the rated voltage and current outputs. The key characteristic of a solar cell is that, whenever its temperature increases, the open circuit voltage deceases while the short circuit current increases marginally. The combined effect is a decrease in power [26].

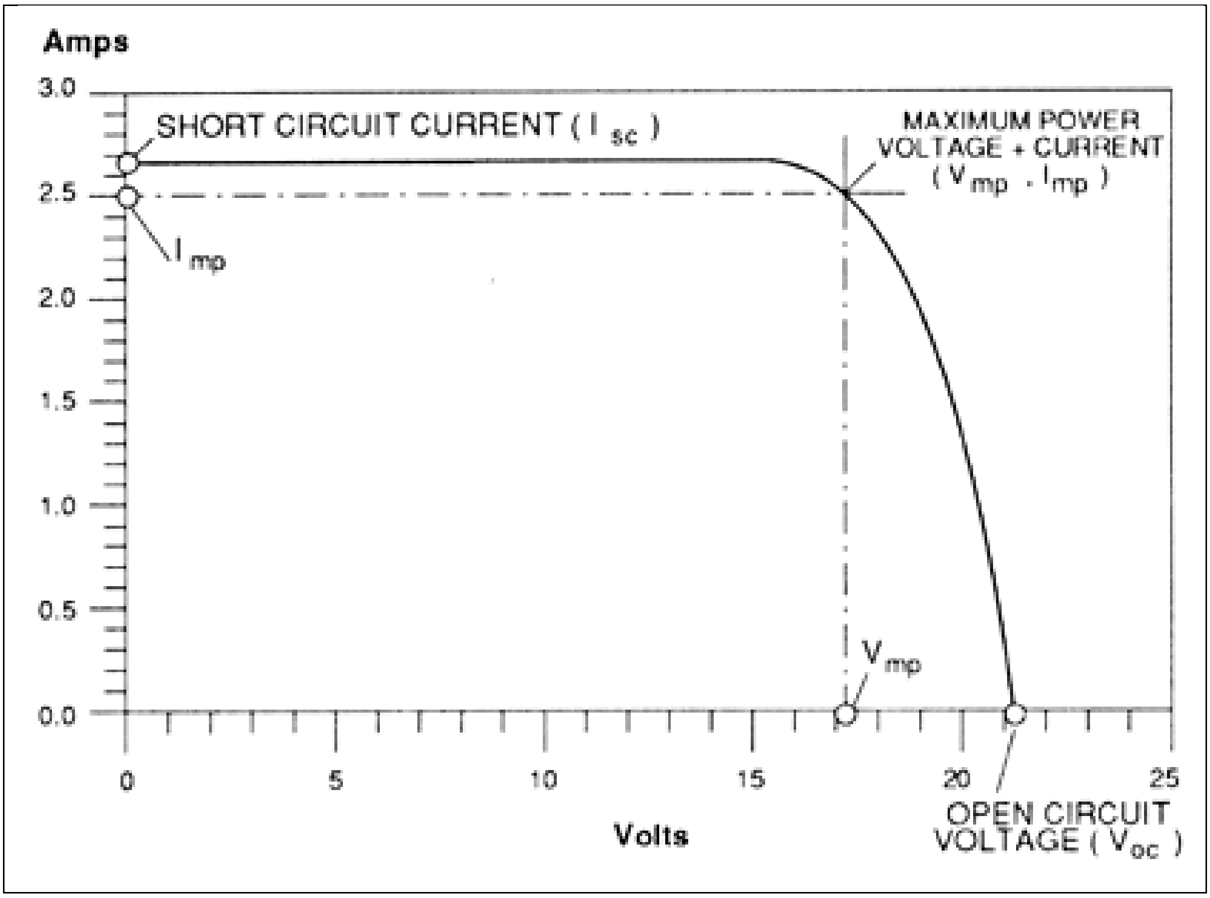

Figure 5: A typical current voltage curve of a PV module [27]

Solar Inverter

The variable direct current (DC) output of the photovoltaic (PV) array is converted to utility frequency alternating current (AC) by a device known as the inverter so that it can either be fed into a national electrical grid or used by a local, off-grid electrical network. An inverter is a major component of a photovoltaic system acting as a critical balance of system that allows the use of ordinary AC-powered appliances [28].

The photovoltaic array yields direct current (DC) as an output, having a challenge of being supplied directly to the appliances that require an alternating current (AC). The solar inverter acts as the core junction among the loads, photovoltaic system as well as the distribution network. Another important characteristic of a solar inverter is that it has peculiar functions such as maximum power tracking as well as anti-islanding protections adapted for their use with photovoltaic arrays. The performance of a photovoltaic mini-grid system is highly influenced by an inverter used. Inverters are of two fundamental classes used in mini grid-connected photovoltaic systems with battery back-up [28].

In order to supply the AC grid, some PV inverters convert direct current (DC) from the array into an alternating current (AC) since they do not directly charge batteries. At times when the PV array produces excess power, the battery inverter-chargers charge the batteries while at times when there is power deficit from the PV arrays, the battery inverter-chargers discharges the batteries. The peak load capable of being connected to the system at any given time is determined by the size of the inverter[28].

Solar Batteries

In order to ensure continuous power supply to the load even under varying environmental conditions, batteries are required in hybrid power generation systems or PV stand alone in order to store the electrical energy during sunshine hours, to be used in non-sunshine hours. The choice of the appropriate batteries to be used in a solar PV system is done with much consideration of their frequency of charging and discharging. For PV applications, the most preferred batteries are lead acid batteries due to them having longest life and least cost per amp-hour while for remote applications where there is need for free maintenance, Gel type lead acid batteries are the preferred ones [29], [30].

For portable applications Nickel-Cadmium or Ni-Metal hydride batteries are used. The life time of the batteries varies from 3 to 5 years. The life time depends on charging/discharging cycles, temperature and other parameters. As outlined by Jossen et al. [29], battery characteristics such as low cost, long life time, high energy efficiency, wide operating temperature, low maintenance and good reliability as well as self-discharge are considered as key when the PV applications are to be designed.

2.2.2 Different kinds of mini-grids

Mini-grids are classified into five power sources comprising, diesel based generators, biomass, mini-hydro, wind, solar photovoltaic (PV) and a hybrid system which is referred to as a combination of two or more of the aforementioned technologies. Up to date, rural electrification resulting from mini-grids development is still based mostly on diesel for electricity generation, though, recent technological improvements as well as solar PV price decline are amongst clear factors showing that in near future, solar mini-grids are likely to outpace and completely replace generator diesel based mini-grids in developing countries.

Thus, equipping the mini-grid development with renewable energy mixtures contributes to energy security enhancement, cost reduction and ultimately minimizes environmental pollution [4].

Hybrid systems are categorized into two streams called grid connected and standalone. Grid connected systems are appropriate in locations close to the electricity grid while standalone systems are those systems where power generation is truly decentralized and they are ideal for remote locations. Sizing the standalone systems is done based on the required local demand, giving thought to the low load factors of the remote locations. The standalone systems differ from the grid-connected systems as they require methods of energy storage, energy backups and advanced power electronic control unlike grid connected where there is a support from the grid during a surplus or surge [31].

2.2.3 Solar PV Mini-grid

Solar PV mini-grid is made up of multiple arrays of PV panels that capture radiation from the sun to generate electricity that is distributed to the households, businesses, and institutional levels for multiple functions [32]. Literature outline that solar mini-grid systems have a ranging capacity of 10-100 kW at village-scale, typically greater than capacity of solar home systems (SHS). The generated electricity is distributed locally after being converted to AC quality typically for a limited number of hours [33].

Energy demand data analysis performed for a local community where the solar mini-grid is to be developed predict the number of solar panels required for such a mini-grid. As outlined by Ulsrud et al. [33], the properly designed solar mini-grid has a capability of supplying needed electricity to serve community requirements (like street water pumping, lighting, schools, and vaccine refrigeration), domestic applications and commercial activities such as communication centers, small mills, and shops.

This kind of a system is called a stand-alone solar photovoltaic system because it consists of only PV energy technology to produce electricity [34]. In order to maintain a continuous supply of electricity in hours where no sun shine is unavailable, solar PV mini-grid constitutes a collection of storage batteries to store energy to be used when the PV produce insufficient energy needed by the load [35].

A proper illustration of a typical solar photovoltaic mini-grid system is as shown in figure 6

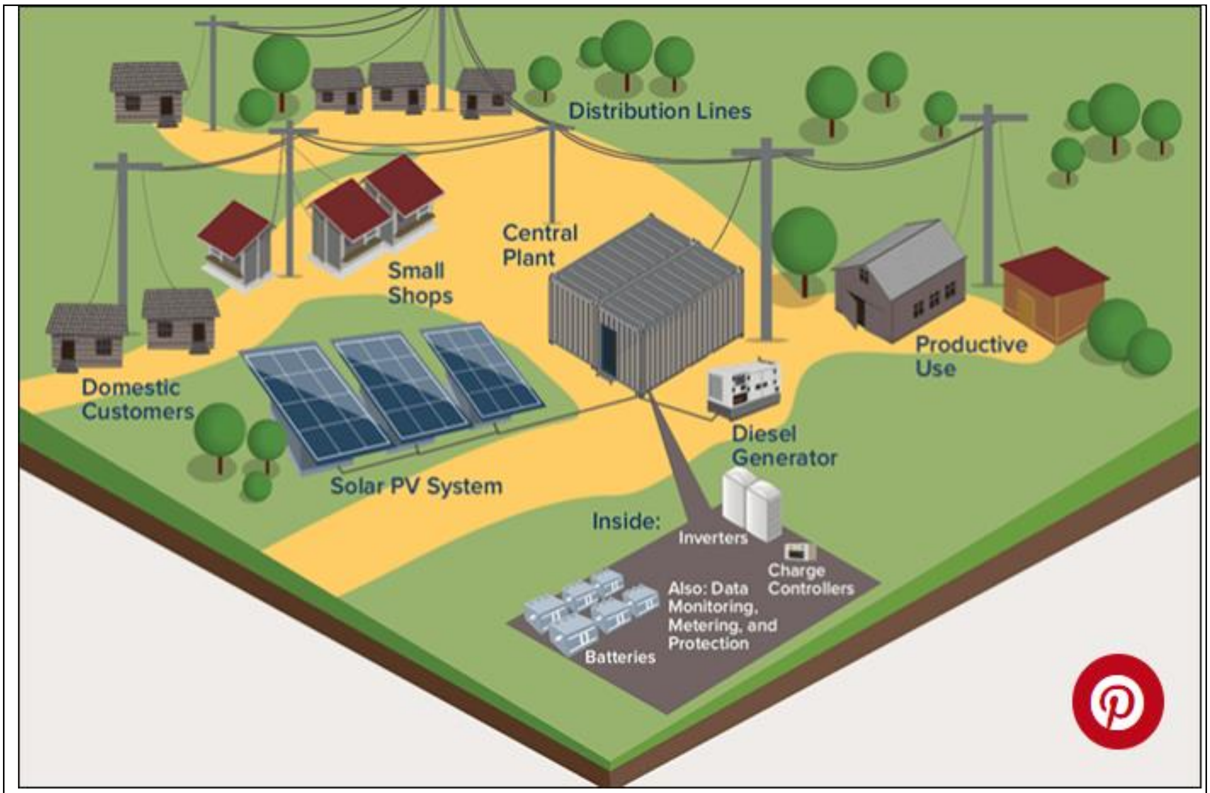

Figure 6: How a typical solar photovoltaic mini-grid system serve communities[36]

2.3 Solar Mini-grid architectural structures

PV/Diesel Hybrid Systems

In a PV-diesel hybrid system, the total power needed by the community is provided through combination of two energy generators being photovoltaics and diesel-based generator. Renewable energy source such as solar is preferred in a hybrid to generate minimum of 75% of total energy demand. This serves as a major advantage for renewables since this makes their application completely independent and also offer lower energy prices as well as future environmental benefits. In a PV-diesel hybrid system, the diesel backup system is dispatched if and only if the load demands surpass the PV capacity. This kind of mini-grid architectural combination ensures better power supply reliability at an affordable manner since it constitute more energy sources. A properly designed solar mini-grid entails PV model, diesel generator, and an inverter [37].

PV/Diesel/Battery Hybrid Systems

The PV/diesel/battery hybrid systems comprise of renewable energy resource (PV), diesel back up along and the energy storage. The presence of storage batteries in this type of a system is very key since it paves a way to conserve the excess energy generated which will later be used whenever load demand surpass the PV capacity as well as during peak hours, thus minimizing frequent intervention of the diesel generator. Another advantage of this kind of architectural combination is that it prevents the diesel generator operating on low loads inefficiently. This is however not actually saying this is a best architectural combination since that is always determined over the cost of generated electricity [37].

PV/Battery Hybrid Systems

This type of solar mini-grid architectural combination consists of the photovoltaic and the storage battery. This combination was earlier recommended as it does not use the diesel generator which is found to lessen the overall project sustainability as well as being harmful to the environment. This kind of mini-grid architectural combination ensures better power availability and supply reliability at an affordable manner since it constitute energy storage batteries. This energy storage of the hybrid system is found to be sufficient so as to conquer power quality problems [11].

2.4 Solar energy resource

The solar energy is determined by solar irradiation received on the geographic location together with local issues like shading and tilting of the arrays. Solar resource assessment is initially done based on satellite data or other sources such as meteorological data. Ground-based measurements are desirable to provide an increased level of confidence as the project develops [38].

2.5 Solar Radiation data

Solar radiation data is generally described in terms of total solar radiation according to Duffie and Beckman [39]. Solar radiation is a combination of beam radiation, which is the solar radiation received from the sun without having been scattered by the atmosphere, diffuse radiation, which is the received solar radiation after the scattering by the atmosphere and ground reflected radiation. Solar radiation is measured mostly on horizontal surfaces by local meteorological stations. As stated by Okundamiya et.al, solar radiation can also be observed through satellites. The major advantage of local meteorological measurements is that more accurate estimates are obtained since they incur the site specific characteristics [39]–[41].

In order to capture maximum solar radiation on earth, surfaces responsible for harnessing solar radiation are usually tilted. The most challenge with this practice is that there is a worldwide deficiency of solar radiation data on tilted surfaces since most of the solar radiation measurements available are only reported for horizontal surfaces [42]. Now, as outlined by Jakhrani et.al [40], solar radiation on tilted surfaces is determined using the empirical models from horizontal surface solar radiation. These models require an extensive evaluation in order to demonstrate their appropriateness considering the local environmental conditions since they are all formulated with the use of dissimilar elements being under different procedures [40], [43], [44].

2.6 Solar radiation on tilted surfaces

In order to design photovoltaic energy systems, simulation as well as evaluating their performance, solar radiation on tilted surfaces critically and appropriately need to be predicted. There exists a number of transposition models of which have been proposed in the literature; and there are ample evaluation studies [45].

The total solar radiation on tilted surfaces is the sum of radiation streams composed of beam radiation, diffuse radiation as well as ground reflected radiation [46].

$$\boldsymbol{I_t = I_{t,b} + I_{t,d} + I_{t,r}} \ldots\ldots\ldots\ldots\ldots\ldots\ldots\ldots (1)$$

Where,

$I_{t,b}$= beam radiation

$I_{t,d}$= diffuse radiation

$I_{t,r}$= radiation reflected by the ground

The diffuse radiation also constitutes three parts known as isotropic part, which is the radiation uniformly received from the whole sky dome; the circumsolar diffuse, which is part of the radiation concentrated around the sun, resulting from solar radiation forward scattering and lastly; the horizon brightening, which is that part of radiation concentrated near the horizon [39], [47].

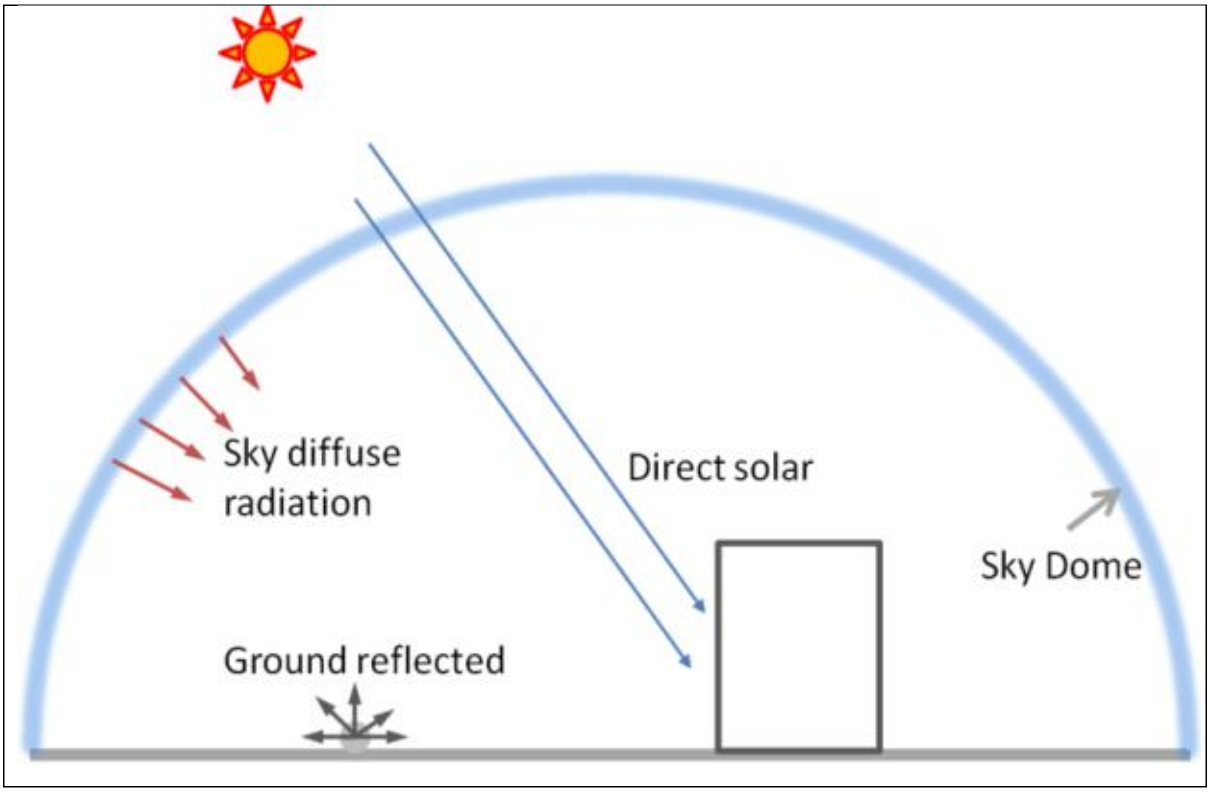

Figure 7: The distribution of diffuse radiation over the sky dome [39]

Including the three components of diffuse radiation in equation 1, the total solar radiation on tilted surfaces becomes:

$$\boldsymbol{I_t = I_{t,b} + I_{t,d,iso} + I_{t,d,cs} + I_{t,d,hz} + I_{t,r}} \quad \ldots\ldots\ldots\ldots\ldots.. (2)$$

Where,

$I_{t,b,iso}$= isotropic part of diffuse radiation

$I_{t,b,cs}$= circumsolar part of diffuse radiation

$I_{t,b,hz}$= horizon brightening part of diffuse radiation

Now, according to Duffie and Beckman [39], beam radiation received on an inclined surface from the horizontal surface is determined as the product of direct horizontal irradiation I_b and the geometric factor R_b which is the ratio of the beam radiation on tilted surface to that on a horizontal surface, represented mathematically as:

$$\boldsymbol{R_b = \frac{I_t}{I} = \frac{cos\theta}{cos\theta_z}} \quad \ldots\ldots\ldots\ldots\ldots\ldots\ldots\ldots\ldots\ldots\ldots\ldots\ldots (3)$$

Where,

$cos\theta$= beam radiation on a tilted surface

$cos\theta_z$= beam radiation on a horizontal surface

Thus,

$$\boldsymbol{I_{t,b} = I_b R_b} \quad \ldots\ldots\ldots\ldots\ldots\ldots\ldots\ldots\ldots \text{(4)}$$

The ground reflected radiation on tilted surface $I_{t,r}$, as stated by Jakhrani et.al [48] is composed of diffuse reflectance ρ_g from the ground (mostly known as albedo) and a view factor F_{c-g}, which is expressed as:

$$\boldsymbol{I_{t,r} = I\rho_g F_{c-g} = I\rho_g \left(\frac{1-cos\beta}{2}\right)} \ldots\ldots\ldots\ldots\ldots\ldots\ldots\ldots\ldots \text{(5)}$$

The empirical models helps in computing the diffuse radiation $I_{t,d}$ and now in order to determine the beam radiation I_b, diffuse radiation is subtracted from the total radiation I_t. All these models used to predict the diffuse radiation on a tilted surface are categorized into two major classes known as isotropic and anisotropic sky models. The difference between the two classes is that isotropic models assume uniformity of diffuse sky radiation intensity over the sky dome regardless of orientation whereas the anisotropic models computes their calculations taking into account the circumsolar diffuse and/or the horizon brightening components on a tilted surface. Thus, the diffuse radiation that is incident on a sloped surface is determined by a fraction of the sky dome seen by it [48], [49].

2.7 Description of some models appropriate for predicting radiation on tilted surfaces

Liu and Jordan Model (1963)

The assumption made in this model is that solar radiation on tilted surface consists of the beam, diffuse and ground reflected radiations. The diffuse radiation is assumed to be completely isotropic, taking both circumsolar and horizon brightening components to be zero [39], [46]–[48], [50]. Thus,

$$\boldsymbol{I_{t,d} = I_d \left(\frac{1+cos\beta}{2}\right)} \ldots\ldots\ldots\ldots\ldots\ldots\ldots\ldots\ldots\ldots\ldots\ldots \text{(6)}$$

Where, β is the tilt angle of the PV array.

Now, the total solar radiation on tilted surfaces using this model is given as:

$$I_t = I_b R_b + I_d\left(\frac{1+cos\beta}{2}\right) + I\rho_g\left(\frac{1-cos\beta}{2}\right) \qquad (7)$$

Temps-Coulson Model (1977)

The model suggested an anisotropic modification to the clear sky diffuse radiance model. The model used clear sky measurements to demonstrate the anisotropic nature of diffuse irradiation [50]. Thus, Temps and Coulson's clear sky irradiance model can be expressed as:

$$I_d = cos^2\left(\frac{\beta}{2}\right)\left[1 + sin^3\left(\frac{\beta}{2}\right)\right]\left[1 + cos^2\theta sin^3\theta_z\right] \qquad (8)$$

Klucher Model (1979)

The model discovered that the isotropic model yields acceptable results for overcast skies though it underestimates irradiance under clear and partly overcast conditions, in particular under increased intensity near the horizon and in the circumsolar region of the sky [47], [50], [51]. The model thus gives the solar radiation on a tilted surface as shown in equation 9.

$$I_t = (I_b + I_d A)R_b + I_d\left(\frac{1+cos\beta}{2}\right)\left[1 + F' sin^3\left(\frac{\beta}{2}\right)\right]\left[1 + F' cos^2\theta sin^3\theta_z\right] + I\rho_g\left(\frac{1-cos\beta}{2}\right) \qquad (9)$$

Where $F' = 1 - \left(\frac{I_d}{I}\right)^2$ is the clearness index.

The horizon brightening is represented by the first of the modifying factors in the sky diffuse component with the circumsolar radiation represented by the second of the modifying factors. The model reduces to the isotropic model under overcast skies because the clearness index F' becomes zero.

Koronakis Model (1986)

The major input of this model was to modify the isotropic sky diffuse radiation assumption by suggesting that the slope $\beta = 90^o$issue 66.7% of diffuse solar radiation of the total sky dome. The view factor (F_{c-s}) was considered to be equal to $[2 + cos\beta]/3$ [46], [48]. Equation 10 now outlines the total solar radiation on a tilted surface using this model.

$$I_t = I_b R_b + I_d\left(\frac{2+cos\beta}{3}\right) + I\rho_g\left(\frac{1-cos\beta}{2}\right) \qquad (10)$$

Badescu Model (2002)

In this model by Badescu for the solar diffuse radiation on a tilted surface, the view factor (F_{c-s}) was considered to be equal to $[\boldsymbol{3+cos2\beta}]/\boldsymbol{4}$ [46], [48]. Hence the total solar radiation on a tilted surface is demonstrated as in equation 11.

$$\boldsymbol{I_t = I_b R_b + I_d \left(\frac{3+cos2\beta}{4}\right) + I\rho_g \left(\frac{1-cos\beta}{2}\right)} \quad (11)$$

Hay and Davies Model (1981)

In this model, the diffuse radiation components considered are isotropic and circumsolar while the horizon brightening is not considered [47], [48].

$$\boldsymbol{I_t = (I_b + I_d A)R_b + I_d \left[\left(\frac{1+cos\beta}{2}\right)(1-A) + AR_b\right] + I\rho_g \left(\frac{1-cos\beta}{2}\right)} \quad (12)$$

Where $\boldsymbol{A = \frac{I_{bn}}{I_{on}}}$ is the anisotropy index. A represents the transmittance through atmosphere for beam radiation. The anisotropy index is used to quantify a portion of the diffuse radiation treated as circumsolar with the remaining portion of diffuse radiation assumed to be isotropic. The circumsolar component is assumed to be from the sun's position.

Reindl et.al Model (1990)

This model by Reindl take into account the horizon brightening and employs the same definition of the anisotropy index A as demonstrated in Hay and Davies model [47], [48], [50]. Representation of the total irradiance on a tilted surface under this model is shown in equation 13 as follows:

$$\boldsymbol{I_t = (I_b + I_d A)R_b + I_d \left\{\left(\frac{1+cos\beta}{2}\right)(1-A)\left[1 + \sqrt{\frac{I_b}{I}} sin^3\left(\frac{\beta}{2}\right)\right] + AR_b\right\} + I\rho_g \left(\frac{1-cos\beta}{2}\right)} \quad (13)$$

The ground reflectance is treated same way as in the isotropic model. Reindl model provides slightly higher diffuse irradiances than the Hay–Davies model since it entails an additional term as shown in equation (13) that takes into account horizon brightening.

Muneer Model (1990)

The model focuses on treating both shaded and sunlit surfaces separately, as are overcast and non-overcast conditions of the sunlit surface [47]. The total solar radiation on a tilted plane for surfaces in shade and sunlit surfaces under overcast sky conditions is given in equation (14).

$$\boldsymbol{I_t = I_b R_b + I_d T_F + I\rho_g \left(\frac{1-cos\beta}{2}\right)} \quad \text{.......... (14)}$$

Sunlit surfaces under non-overcast sky conditions can be determined using equation (15) illustrates as:

$$\boldsymbol{I_t = I_b R_b + I_d [T_F(1-A) + AR_b] + I\rho_g \left(\frac{1-cos\beta}{2}\right)} \quad \text{.......... (15)}$$

Where, T_F is the ratio of the slope background diffuse irradiance to the horizontal diffuse irradiance and it is represented mathematically as follows:

$$\boldsymbol{T_F = \left(\frac{1+cos\beta}{2}\right) + \frac{2B}{\pi(3+2B)}\left[sin\beta - \beta cos\beta - \pi sin^2\frac{\beta}{2}\right]} \quad \text{.......... (16)}$$

The values of the radiation distribution index B depend on the particular sky and azimuthal conditions, and the location.

Perez et.al Model (1990)

The Perez model is more computationally intensive and based on a three components treatment of the sky diffuse irradiance. The model represents more detailed analysis of the isotropic diffuse, circumsolar and horizon brightening radiation by using empirically derived coefficients [47], [50], [52]. The total solar radiation on a tilted surface using this model is given as shown in equation (17).

$$\boldsymbol{I_t = (I_b + I_d A)R_b + I_d\left\{(1-F_1)\left(\frac{1+cos\beta}{2}\right) + \left[F_1\frac{a}{b} + F_2 sin\beta\right]\right\} + I\rho_g\left(\frac{1-cos\beta}{2}\right)} \quad \text{.......... (17)}$$

Where F_1 and F_2 are respectively circumsolar and horizon brightening, a and b are the terms responsible for taking into account the incidence angle of the sun on the considered slope.

$$\boldsymbol{a = max(0^0, cos\theta)}$$

$$\boldsymbol{b = max(cos85^0, cos\theta_z)}$$

The two brightness coefficients F_1 and F_1 are functions of the sky condition parameters known as clearness ε and brightness Δ given by:

$$\varepsilon = \frac{\frac{I_d+I_n}{I_d}+5.535x10^{-6}\theta_z^3}{1+5.535x10^{-6}\theta_z^3} \quad (18)$$

$$\Delta = m\frac{I_d}{I_{on}} \quad (19)$$

Where, where m is the air mass and I_{on} is the extraterrestrial normal-incidence radiation.

Now, F_1 and F_2 are computed as illustrated in equations (20) and (21)

$$F_1 = max\left[0,\left(f_{11} + f_{12}\Delta + \frac{\pi\theta_z}{180}f_{13}\right)\right] \quad (20)$$

$$F_2 = f_{21} + f_{22}\Delta + \frac{\pi\theta_z}{180}f_{23} \quad (21)$$

The coefficients f_{21}, f_{21}, f_{21}, f_{21}, f_{21} and f_{21} according to the model were derived based on a statistical analysis of empirical data for specific locations.

HDKR (Hay, Davies, Klucher, Reindl) Model (2006)

This model is the combination of Hay and Davies, Klucher and Reindl models. It combines all terms of diffuse radiation known as isotropic, circumsolar and horizon brightening to the solar radiation equation in order to develop a new correlation known as HDKR model [39], [48]. The total solar radiation on tilted surface is thus determined as:

$$I_t = (I_b + I_d A)R_b + I_d\left\{(1-A)\left(\frac{1+cos\beta}{2}\right) + \left[1 + sin^3\left(\frac{\beta}{2}\right)\right]\right\} + I\rho_g\left(\frac{1-cos\beta}{2}\right) \quad (22)$$

2.8 Studies conducted that compared performance of different models

In Lesotho, an investigative study by Gopinathan K.K [53] concentrated on solar radiation on diversely oriented sloping surfaces using the isotropic model suggested by Liu and Jordan. Conclusions pertaining the optimum tilt as well as orientation for winter, summer and annual collection were reached. A study by Shukla et al. [54] conducted in India compared the performance of isotropic and anisotropic sky models that are used to estimate the amount of solar radiation incident on the sloped surfaces. The conclusion reached was that the excessive solar radiation for the entire year was estimated by Hay and Davis model and on the other hand, among all isotropic and anisotropic models, Badescu model provided the lowest solar radiation.

Comparison of modelled and measured tilted solar irradiance for photovoltaic applications was conducted by Mubarak et al. [55] using five empirical models. The output of that study outlined that models of Hay and Davis and Reindl are best for estimating sloped irradiance for south-facing modules for climate conditions that are mostly cloudy and also measurements for ground reflectance not being available. On the other hand, Perez model was found to be ideal for sunny places with measurements of ground reflectance available. In order to estimate direct normal irradiance for Korea, Lee et al. [56] analyzed ten solar radiation models and a conclusion was reached that Reindl model is the best over the models analyzed for Korea.

In Belgium, the performance of 14 empirical models were assessed by Demain et al. [57] in order to predict solar radiation from horizontal to tilted surfaces. Different models' respective performance under different sky conditions were investigated and it was found that statistical validation procedures disclosed that none of the studied models was best under all kinds of sky conditions which led into development of a hybrid model from the coupling of three models.

An investigative study on the accuracy of different empirical models used for estimating solar radiation on a tilted surface was carried out by Despotovic et al. [58] with the aim of assessing as well as comparing performance of available models in the literature. The study used statistical analysis in order to evaluate the performance of those models by using long term measurements at different sites.

2.9 Estimation of the module Cell Temperature

The operating temperature of the photovoltaic (PV) module is amongst the most fundamental parameters after solar radiation for the long term evaluation of PV systems since it modifies the power output and system efficiency. The temperature of the module is a function of many parameters such as solar radiation, air humidity, ambient temperature, speed and direction of the wind, photovoltaic module orientation, dust and sand deposition on PV module, and PV module materials. In view of these, it is advisable, for better performance and increasing lifetime of the PV model to always predict its behavior in a particular geographical area where the system is to be installed [59]–[61].

For the proper prediction, characterization of the behavior of PV modules at any location is done with the use easiest and acceptable tools known as models. As outline in Jatoi et al. [60], the module temperature is affected by weather conditions, hence it is very key to quantify its influence. Modeling is the quick help as it eventually guides in proper design of the better systems for better functioning. Different authors from different countries have made multiple attempts to demonstrate by virtue of examples the behavior of PV modules. Categories of the used models for predicting module temperature is divided into steady-state or dynamic and explicit or implicit. All parameters in steady-state modeling are taken to be independent of time though those models are useful for specific locations and module technologies. Dynamic models have some parameters which varies with time [60], [62], [63].

It is however, very important to select an appropriate model for the design and sizing of photovoltaic systems so as to avoid faulty predictions which will in turn make an over- or undersized system. The major disadvantage of an oversized system is that it becomes very costly while that of an undersized system is that it causes malfunctioning of the system since the system fails to supply critical loads [61]. Most studies on PV module temperature are conducted using the nominal operating cell temperature (NOCT) model or the Sandia National Laboratory (SNL) model [64]. Garcia and Balenzategui [65] stated that the NOCT model of the photovoltaic module temperature is one of the simplest models because it depends only on solar radiation and ambient temperature.

It was outlined by Garcia and Balenzatengui [65] that SNL model is more accurate as opposed to NOCT model since it also considers wind speed, PV module type and configuration of its installation. Nevertheless, several conducted studies were performed with different parameters considered such as solar radiation, ambient temperature and wind speed at different places and that resulted in development of different formulas [66], [67].

2.10 Existing PV Module Temperature Models

A conducted study by [68] focused only on one climatic variable which is ambient temperature. The limitation of this method was found to be lack of reflection of the whole behavior of the environment since it uses one input variable. Equation 23 illustrate the developed model and it was also used by [69].

$$\boldsymbol{T_c = 1.411T_a - 6.414} \quad (23)$$

As stated by Hove. 2000[70] in his model, efficiency of a PV array is a function of cell temperature and array irradiation illustrated as follows:

$$\boldsymbol{\eta = \eta_r[1 - \beta(T_c - T_r) + \gamma log_{10}I_{array}]} \quad (24)$$

Where η_r is the array efficiency measured at reference cell temperature, β is a temperature coefficient, T_c is the cell temperature, T_r is the reference cell temperature at which η_r is determined, γ is a radiation-intensity coefficient for cell efficiency and I_{array} is the radiation incident on the array per unit area. Adopting $\gamma = 0$, as well as considering the energy balance of the array, the model predicted cell temperature as shown in equation 25:

$$\boldsymbol{T_c = T_a + 0.9\left(\frac{T_{c,NOCT} - T_{a,NOCT}}{I_{array,NOCT}}\right) I_{array}} \quad \ldots\ldots (25)$$

The model proposed by Muzathik[71] suggested three variable models being the ambient temperature T_c (°C), global solar radiation G_{sr} (w/m^2), and wind speed W_v m/s. Illustration of this model together with coefficients of each variable are given in equation 26.

$$\boldsymbol{T_c = 0.943T_a + 0.0195G_{sr} - 1.528W_v + 0.3529} \quad \ldots\ldots (26)$$

Another model that considered the three variable ambient temperature, global solar radiation as well as wind speed was proposed by [62]. This model is demonstrated in equation 27 and it is simple and semi-empirical model for the calculation of module temperature.

$$\boldsymbol{T_c = T_a + \left(\frac{0.25}{5.7 + 3.8W_v}\right) G_{sr}} \quad \ldots\ldots (27)$$

Photovoltaic module temperature was calculated using an illustrated model in equation 28 developed by Duffie and Beckman [39]. The model calculate the cell temperature in controlled nominal operating cell temperature (NOCT) conditions known to be 800 w/m^2 solar radiation, 20°C ambient temperature and 1 m/s wind speed. This model is also adopted by [60] with T_a , G_{sr}, and NOCT conditions as illustrated in equation 28 .

$$\boldsymbol{T_c = T_a + \left(\frac{0.25}{5.7 + 3.8W_v}\right)\left(\frac{G_{sr}}{G_{sr-NOCT}}\right)(T_{c-NOCT} - T_{a-NOCT})\left[1 - \frac{\eta_c}{\tau\alpha}\right]} \quad \ldots\ldots (28)$$

2.11 Load Demand Assessment

There are several characteristics of the rural areas that distinguish them from the entire world. Rural communities particularly in the developing countries, are composed of substitutable folks or those that haven't however become a region of the fast-paced exterior world. Power unavailability in rural areas, have tailored folks to a more natural and organic living with standard ways and ancient approaches. Therefore, the expected energy consumption of a remote rural area may be completely different from that of an urban area[72].

An exact pattern of electricity demand estimation for a newly electrified community is very tricky to develop because of absence of suitable records of existing load profiles found for most if not all rural communities. This is brought by the fact that they are dispersed, less crowded with low power requirements, thus keeping them away from such record analysis. An alternative approach mostly used to estimate the demand is that of considering any comparable community powered by a community-owned diesel generator so as to conveniently measure as well as relate produced electricity to that of the targeted community. If there isn't any community powered by diesel generator for comparison purposes, then appliances having a potential of being used as soon as the mini-grid is developed are thus used to develop a load curve[72], [73].

The community's energy demand and pattern is influenced by a number of different factors including among others the number of households together with the number of people residing per household, kind and time of use of the appliances that are being used as well as seasonal variations. Energy demand demonstration can be defined either for the entire community or for each household on a daily, monthly and annual basis. A more detailed, at most accurate and realistic load curve for the community involves taking into consideration two types of demand known to be private household electricity demand and demand from public facilities[74].

The demand curve is mostly influenced by different working days and weekends as well as the seasons of the year. For studies where the mini-grid is developed in rural areas where people there are exposed to electricity for the first time, mostly distinction between working days as well as weekends seems to be irrelevant since mostly people residing in those communities are mainly farmers whom are working every day[73], [74].

A number of different studies conducted particularly for rural households in Africa outlined a monthly 50 kWh up to 125 kWh per month range in energy demand estimate for a household in rural Africa. Each household experiences a different consumption due to its affordability as that differs significantly between households as well as different communities. Scenarios for total demand on mini-grids are obtained via classification of rural households by the size, given their total electricity consumption of rural households. A clear sign of required energy generation is fundamental for successful choice of technology and system design[75].

The above stated load assessment was only considering households' consumption. Whenever a mini-grid is developed in a community, productive use of energy is encouraged to people within that community as well as introduction of some industries. The consumption from the households is much smaller as compared to the one represented by the contribution from the productive or industrial uses of electricity. In the presence of industries, the total power consumption is influenced by them, whereas productive use mostly need power during the day. This now makes the daytime peak load from the productive use not to easily surpass that of private households in the evening. Thus project developers are always anticipated to clearly evaluate load constituted by productive users on the mini-grid[75], [76].

2.12 Solar PV system power output prediction

Proper sizing of the photovoltaic systems involves a sophisticated prediction of the solar PV array power at any given time, characterized by given meteorological conditions. The reason behind this is that PV module electrical power output is variable and responds to the time-step variation of meteorological conditions such as solar irradiance, ambient as well as the wind speed. The electrical output power of the PV array is found to be proportional to the solar irradiance at any given size. The opposite happens with the ambient temperature as well as the wind speed since at high solar irradiance level drives up the cell temperature, giving rise to reduction of the conversion efficiency of solar radiation to electrical energy [70].

It is thus mandatory to know the time-step variation of the solar irradiance as well as the PV cell temperature as influenced by the ambient temperature, the wind speed and the way the solar module is mounted.

2.13 Diesel generator output

The output power of the diesel generator (DG) is either zero (meaning DG is switched off) or DG rated power (DG switched on) at any selected hour. When designing the PV system with backup diesel generator, the embraced DG energy dispatch strategy is fundamental for providing the conditions for switching on or off. Three DG energy dispatch strategies namely night dispatch strategy, load following strategy and cycle charging are discussed in detail as follows [77]:

a) The night dispatch strategy

In this strategy, assumption made is that the diesel generator is switched on during the night only due to absence of solar radiation. This strategy is ideal and user friendly as it is easier to operate since it does not use complicated electronic control, though it is considered wasteful for load profiles exhibiting low night energy usage.

b) The load-following strategy

Whenever the load is equal or exceeding a prescribed threshold, the strategy switches the diesel generator ***ON***. Unlike the previously discussed strategy, the load following strategy is regarded as a more economical since it is dispatched if and only if there is a need, resulting in a diesel generator operating at high load factors which give rise to low specific fuel consumption and longer diesel generator lifespan. The major disadvantage of this strategy is that costly electronic controls need to be used for its implementation which in turn are also difficult to maintain.

c) Cycle charging strategy

In this strategy, the diesel generator is switched ***ON*** so as to cover the net-load demand as well as charging the battery. As along as the diesel generator is within its stipulated run time, it will continue running until either one of the following conditions is met:

- The stipulated state of charge of the battery set point has been met, or PV power is enough to satisfy the load.
- The renewable power is sufficient to meet the load as well as continue to charge the batteries.

2.14 Economic Analysis on PV System

Developing and implementing a project requires a thorough determination of the profitability of a project. This is done in several ways with the most common methods used to examine the profitability of a solar photovoltaic project being payback period, net present value, net cash flow (NCF) as well as the internal rate of return (IRR). These different methods are described in details in order to identify the most appropriate one to be used in particular for a solar PV project [78].

2.14.1 Payback

Payback period is described in simpler terms as the maximum required number of years needed to recover the original investment. A project is classified to be best if the payback period is very short as that enables investors to quickly recover their invested capital. Shorter payback period is very advantageous since it minimizes the project's future risks arising from the expected future cash flows. As advantageous as it may be, payback period method still encounters some flaws when used to determine the project's effectiveness in an investment [79].

Here are some of this limitations: It only considers benefits before the payback period and ignores thereafter benefits, that means that method does not measure profitability. The key objective of the payback period method is on recovering the capital not necessarily focusing on profits [78]. Whatever returns collected after the payback period are not considered by this method suggested by [79]. Illustrated in equation 29 is the payback period equation.

$$\boldsymbol{Payback\ period = year\ before\ full\ recovery + \frac{unrecovered\ costs\ at\ the\ start\ of\ the\ year}{cash\ flow\ during\ the\ year}} \quad (29)$$

2.14.2 Net present value calculation

The way in which an investment project affects the wealth of the shareholders of the company presently is outlined using a strategic method known as the Net Present Value (NPV). NPV can be both positive or negative. A positive NPV shows that shareholders' wealth is enhancing and highly appreciated while a negative NPV shows that the project is not viable and hence the project cannot be implemented. NPV is calculated as a discount of the future free cash flows using a discount rate which depends on the nature of the project, add the discounted free cash flows through the economic life-time of the project and subtract the overall initial investment from the total [78], [80], [81].

The chosen discount rate should always be capable of enabling the investor to obtain from more or less risk-free investments which is referred to as the internal rate of return (IRR). The discount rate can be high or low depending on the risk levels of the project. Illustrated in equation 30 is the formula used to determine the NPV:

$$NPV = \sum_{n=1}^{i} \frac{CF_n}{(1+r)^n} - I_0 \quad \text{...} (30)$$

Where,

CF_n = Net cash flow in year n

I_0= Initial cost

r = discount rate

n = year number

i = economic life-time of investment

2.14.3 Levelised cost of energy

Currently, it is of great benefit to assess the cost competitiveness of renewable Energy Technologies (RETs). The conclusions pertaining financial viability of a solar photovoltaic power plant arise from determination of the Levelised Cost of Electricity (*LCOE*). The concept known as Levelised cost of energy (LCOE), is an introduced measure used to compare the life-cycle costs of technology options. LCOE depend on the Net Present Value of the total life-cycle cost of the project calculated as per kilowatt-hour (unit cost of energy). A simpler explanation and easy way of determining LCOE is to divide the net present value of the total life-cycle costs by total life-cycle energy production as illustrated by equation 31 [82], [83].

$$LCOE = \frac{Total\ life\ cycle\ costs}{Total\ life\ cycle\ production} \text{.................................} (31)$$

Mostly in literature, an adapted interpretation of LCOE states that it is the total constant price of the project throughout its lifetime at which electricity can be sold. The price is the appropriate one to cover all incurred costs such the investment costs, O&M costs, debt with interests, equipment replacements and a return to investors as well as rent and taxes [83].

2.14.4 Real Levelised Cost of Energy calculation

The real Levelised Cost of Energy (rLCOE) differs from the outlined nominal LCOE in section 2.14.3 calculations since it makes use of real discount rates as opposed to nominal discount rates. The major disadvantage of the rLCOE is that it does not take into account the inflation effect on operation and maintenance (O&M) as well as other issues such as fuel prices hence the nominal LCOE is regarded as an appropriate estimate from the developer's perspective because of its higher level of financial detail yielded by inflation corrections. The inflation effect is significantly very low for renewable energy technologies (RETs) impacting no or a slight influence on LCOE calculations [84].

The rLCOE doesn't only ignore inflation effect, it also pays no attention to the effect of inflation incident on capital costs. Not considering these inflation effects may be of significant effect when it comes to renewable energy technologies since it generally represents high CAPEX levels. Advantage of real is that its estimates are found to provide sufficient financial detail.

$$\boldsymbol{LCOE = \frac{Capex + \sum_{n=i}^{i} \frac{AC}{(1+r)^n} - \frac{AR}{(1+r)^n}}{\sum_{n=1}^{i} \frac{AEP(kWh) * (1-Lf)^n}{(1+r)^n}}} \quad \ldots\ldots\ldots\ldots\ldots\ldots\ldots\ldots\ldots\ldots\ldots\ldots\ldots\ldots\ldots\ldots\ldots\ldots\ldots\ldots\ldots\ldots \text{(32)}$$

Where,

AC = Annual costs

AR = Annual revenue

AEP = Annual energy production

Lf = annual loss factor (system efficiency decrease rate)

Capex = Capital expenditure

n = year number

i = economic life-time of generating system

2.15 System sizing

The process of adequately evaluating both voltage and current ratings for each component of the photovoltaic system to meet the electric demand at the facility and at the same time calculating the total price of the entire system from the design phase to the fully functional system including, shipment, and labor is known as system sizing. This process depends on a variety of factors such as geographical location, solar irradiation, and load requirements. The proper sizing of the main system components of a PV system is crucial in determining both energy supply reliability and cost affordability of the system [85]–[87].

An oversized PV system will unnecessarily increase first-cost and might also be inefficient and reduce system life (e.g. an oversized battery may not fully charge most times, reducing battery life, or an oversized PV module will overheat reducing efficiency and lifespan). On other hand, an undersized PV system will have disappointing energy yield and supply reliability, providing less utility the energy consumer. Off-grid (stand-alone) PV systems are the most challenging in terms of sizing as they have to be autonomous in energy supply [85], [87], [88].

This study discusses two approaches used to size stand-alone PV systems:

1. The average-day energy balance approach and
2. The time-step energy balance approach

The average-day energy balance approach is the simplest one to use. It requires less sophisticated input meteorological data, but is less exact and may lead to over-size and costly PV system. Contrary, the time-step energy balance approach requires time-step (e.g. hourly data) meteorological and load data, which is often not easily available, but is more exact, allows estimation of system energy supply reliability and often lead to a more economical system design. Availability of solar radiation in the average-day energy approach is based on minimum monthly average peak sunshine hours [85].

The electrical energy load is taken as a daily total that does not take into consideration hourly variations. Five main steps are required in order to size the battery bank and the PV array size for the system. More steps may be included for sizing other components such as the inverter and charger controller. In order to determine power consumption demand, the electrical devices available at the residence or capable of being bought are itemized with their power ratings and time of operation during the day to obtain the average energy demand in Watt-hour per day. The total average energy consumption is used to determine the equipment sizes and ratings starting with the solar array and ending with system wiring and cost estimate [85], [87].

2.15.1 Sizing of the Solar Array

Sizing the array requires determination of the total daily energy (E) in Watt-hours (Wh), the average sun hour per day (T_{min}) and the system DC-voltage (VDC). Incurred losses when sizing is taken into account by dividing the total power demand in Wh per day by the product of efficiencies of all components in the system to get the required energy E_r.

$$E_r = \frac{daily\ average\ energy\ consumption}{product\ of\ components'\ efficiencies} = \frac{E}{\eta_{overall}} \qquad (33)$$

The determined energy E_r is divided by the average sun hours per day for the geographical location T_{min} to get the peak power.

$$P_p = \frac{daily\ energy\ requirement}{minimum\ sun\ hours\ per\ day} = \frac{E_r}{T_{min}} \quad (34)$$

Now, with the peak power determined, the total current needed can be calculated by dividing the peak power by the DC- voltage of the system.

$$I_{DC} = \frac{Peak\ power}{system\ DC\ voltage} = \frac{P_p}{V_{DC}} \quad (35)$$

Connection of the PV modules must be either in series and/or parallel according to the need to meet the desired voltage and current. The number of modules to be connected in parallel is determined by equation 36 as follows:

$$N_p = \frac{whole\ module\ current}{module\ rated\ current} = \frac{I_{DC}}{I_r} \quad (36)$$

On the other hand, the number of series modules is determined as shown in equation 37, which equals the DC voltage of the system divided by the rated voltage of each module V_r.

$$N_s = \frac{system\ DC\ voltage}{module\ rated\ voltage} = \frac{V_{DC}}{V_r} \quad (37)$$

2.15.2 Sizing of the Battery Bank

The required energy to be stored is roughly determined to be equal to the multiplication of the total power demand (E) and the number of autonomy days (D) as illustrated in equation 38 [85], [88].

$$E_{rough} = ExD \quad (38)$$

Considering safety majors, the result obtained in equation 38 is divided by the maximum allowable level of discharge (MDOD) to deduce the safe energy (E_{safe}):

$$E_{safe} = \frac{energy\ storage\ required}{maximum\ depth\ of\ discharge} = \frac{E_{rough}}{MDOD} \quad (39)$$

It is at this juncture that each battery rated voltage (V_b) to be used be chosen. Now, dividing the determined safe energy storage required in equation 39 by the DC voltage of one of the batteries selected yield an important parameter known as the capacity of the battery bank needed in ampere hours.

$$C = \frac{E_{safe}}{V_b} \quad \text{.........} \quad (40)$$

The total number of batteries in a battery bank is determined by dividing the capacity C of the battery bank in ampere-hours by the capacity of one of the battery C_b selected in ampere-hours.

$$N_{batteries} = \frac{C}{C_b} \quad \text{.........} \quad (41)$$

Number of batteries connected in series in a battery bank is thus determined by dividing the DC voltage of the system by the voltage rating of one of the selected batteries:

$$N_s = \frac{V_{DC}}{V_b} \quad \text{.........} \quad (42)$$

On the other hand, then number of parallel paths N_p is found by dividing the total number of batteries by the number of batteries connected in series:

$$N_p = \frac{N_{batteries}}{N_s} \quad \text{.........} \quad (43)$$

2.15.3 Sizing of the Inverter

An inverter is used in the system where AC power output is needed. The input nominal voltage to the inverter is the same as the battery voltage. For stand-alone systems, the first thing to be done when sizing the inverter is to determine the actual power drawn from the appliances that will run at the same time. The inverter must be large enough to handle the total amount of power that will be used at one time and is size must be 20–25 % bigger than total power of appliances. On the other hand, chosen inverter must be able to continuously supply power to start any loads that may surge when turned on and particularly if they turn on at the same time [85], [89]. The following steps are used to determine proper inverter ratings:

- AC appliances total power, maximum demand and surge demand should be obtained
- Inverter capacity should be 20–25 % bigger than AC appliances total power

Chapter 3

3. Methodology

This chapter outlines the methodological approach employed to calculate, analyze and optimally simulate information pertaining this study project. Chosen models employed in calculations are well explained as well as the reason behind them being chosen when developing the Microsoft Excel based program that analyze different solar mini-grid architectural strictures and providing the best one in terms of lower Levelised Cost of Energy (LCOE).

3.1 Data Analysis

Analyzing data is the most critical task of this study. This is where energy related data such as solar resource was examined, cleaned as well as modelled with a major target of making informed decisions towards energy efficiency conclusions. Analyzed sets of data in this study include solar radiation data, most likely anticipated loads as well as the forecasted PV system energy yields.

3.1.1 Appliance Power Matrix

Potential electric appliances that can be easily afforded and used by rural communities were selected and the load was analyzed. For realistic purposes, estimates on future growth loads were undertaken paying more attention on energy usage habits and the levels of lifestyle. With reference to SE4ALL prefeasibility study on solar mini-grids reports in Lesotho, appliances that most interviewed rural people outlined as key to have once they are electrified were used to carry out an energy demand analysis with few additional appliances of which people can be encouraged to use for effective/productive use of energy. Power ratings of the appliances as well as number of appliances to be powered by the solar grid are illustrated in detail in table 1 showing how total power consumption is calculated.

Table 1: sample of the appliance power matrix

Appliance	Power Rating	Quantity	Total Power Consumption
A	xx	2	2xx
B	xxx	2	2xxx

C	xxxxxx	1	xxxxxx
D	x	10	10x
E	xx	1	xx

As shown in table 1, the total power consumed by different appliances is the product of its power rating and the number of those appliances.

3.1.2 Appliance time of use scheduling

Appliances that were selected to be powered by the designed solar mini-grid in this study were categorized into four different classes due to their operational behavior as well as considering rural behavior of the communities. Time of use of each appliance was assumed with reference to a typical lifestyle in Lesotho, particularly in the rural areas.

a) Operating cycle of the appliances

Appliances such as refrigerators do not continuously work during their operating time, they automatically turn on and off depending on the inside temperature. This way of operation discards initially stated way of calculating consumed energy in table 1. Direct observation was considered in this regard to provide estimates of the operation/duty cycle.

b) Planned Appliances

These kind of appliances perform only at prearranged times. Examples include computers, lights as well as irrigation systems. In ordered to estimate proper energy consumption of these kind of appliances, this research considered the time factor of which the appliance is used and interconnected it with the established power element of the equipment.

c) Shadow Appliances

Appliances referred to as shadow in this study are those that uses energy even at times when they issue nothing in return. No matter they are switched off, these kind of appliances still consumes power though it is considered to be significantly small. Energy usage distribution within the 24 hours a day were analyzed and demonstrated in a demand matrix, which will in detail explained in sub-section 3.1.3.

d) Starting surge loads

More power is drawn for surge loads than the operating rated power as they consist of a motor that has a surge. that is before the motor is up to its operating speed it draws more than its rated operating power.

The study observed that there are variations in consumption, categorized as daily variations which are associated with weekdays and weekends as well as seasonal variations. For simplicity of this study in computing the load profile, the daily variations were ignored and assumption of constant daily consumption was employed. Lesotho experiences four seasons though also in this case, it was noticed that these seasonal changes have a minimal impact in the energy consumption, hence an assumption that monthly energy demand is maintained constantly throughout the year was also employed.

3.1.3 Demand Matrix

Demand matrix was chosen as a suitable method to calculate the different loads as discussed under appliance time of use scheduling. The time of the day at which an appliance is in operation is shown by the matrix for that particular hour. The percentage number of appliances of similar type that are ***"ON"*** in a particular time is stated, with 1 outlining 100% operation of all appliances of the same kind in a power demand matrix. Table 2 illustrate an example of a computed demand matrix:

Table 2: Demand matrix computation

Day Time in (Hours)	**Appliances(five different appliances chosen)**				
	1	**2**	**3**	**4**	**5**
16:00	0.3	0	0.5	0.2	0.5
17:00	0.3	0	0.6	0.2	0.5
18:00	0.3	0	0.6	0	1
19:00	0.3	0	1	0	1

As already stated, this method computes load behavior for each hour for the entire daily 24 hours. For each appliance, percentage number of appliances that are ***"ON"*** in every hour of the day is multiplied by the power rating of that appliance, summed up for the 24 hours of the day to compute daily energy consumption of that appliance. Now total energy consumption for all appliances is shown as illustrated in table 3.

Table 3: Hourly load profile matrix for Sehong-hong

Hour	Power (kW)
1	15.4583
2	15.4583
3	15.4583
4	15.4583
5	21.3081
6	31.5304
7	39.80239
8	41.39571
9	56.51521
10	56.61751
11	56.66041
12	56.66041
13	56.66041
14	56.66041
15	56.51778
16	40.81308
17	44.79266
18	52.1587
19	44.06299
20	30.31116
21	22.58311
22	20.19677
23	17.88105
24	14.26975
Total daily	**879.2312**

3.1.4 Load Profile

Successful determination of hourly power demand from demand matrix table is key in developing the resulting load profile which is plotted using the instantaneous hourly power demand against time. In developing the load profile, the minimum and maximum average temperatures in Lesotho were assumed to be almost constant throughout the year. The other made assumption was that of rainfall having no impact on local electricity demand in the rainy season. Thus, it was taken as a result a simplifying assumption that the load curve would be the same for any day all year long.

In this study, the load for one of the ten places selected by SE4ALL in Lesotho, namely Sehong-hong in Thaba-Tseka district was computed, with the load divided into three forms namely household, public as well as productive loads. In order to effectively utilize produced energy during the day (avoiding too much dumping), productive us of energy are encouraged to the people by giving them tips on some of the businesses that they can start once the energy is provided to them. The public loads are those associated with either government or private entities such as schools, clinics, etc. Figure 8 illustrates the developed load profile for Sehong-hong.

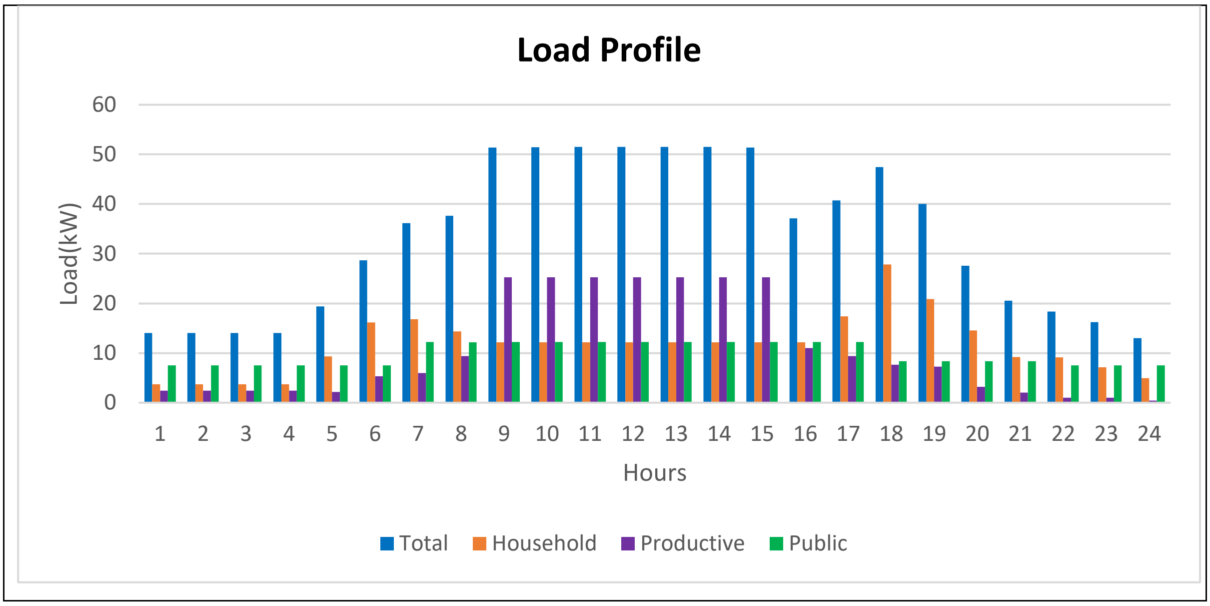

Figure 8: Detailed projected load profile for Sehong-hong

The percentage share of each sector in the overall determined load is illustrated as shown in figure 9. Domestic load constitutes major share of the total demand with 36%, followed by the productive use with 33% and lastly is the public use with 31%.

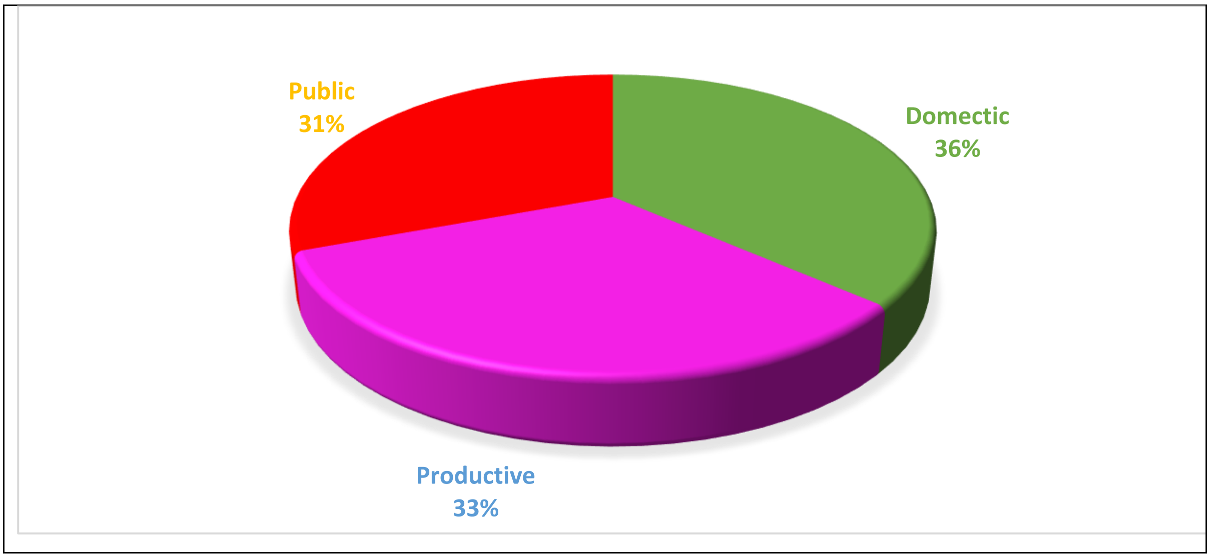

Figure 9: The share of each of the three considered types of the demand

3.2 Resource Analysis

The assessment of the solar resource and its review ranged from simple to complex analysis. For the simple analysis, desktop review which consisted evaluating publicly available data at a high level for the site was carried out for estimating the approximate solar power potential. Complex analysis required an assessment of a combination of data from multiple sources such as long term reference stations which was very challenging since getting data in Lesotho is an unclimbable mountain.

3.2.1 *Measured Data Considerations*

There was no luck in finding the ground measured radiation data from Lesotho Meteorology Services for comparison purposes with the downloaded satellite data. Several attempts were made to meet the person to provide the data but there was no success and thus I had to rely only on the satellite data.

3.2.2 Treatment of Solar Radiation data

A very important task for designing, simulating as well as evaluating the performance of photovoltaic energy systems is to estimate solar radiation on inclined surfaces. Several models have been in the literature with this study picking just ten models, four isotropic and six anisotropic models. The ten models were compared in terms of their performances for their relative merits in estimating diffuse solar radiation on sloped surfaces in Lesotho. Assumptions made in all the models were based on isotropy or anisotropy of the sky conditions.

Grading/ranking the relative ability of the different models to predict the global solar radiation on a tilted surface is not a simple task at all. The performance of the individual models was determined by utilizing both graphical and statistical methods. The HDKR model is strongly recommended for surfaces slope towards the equator. The model is user friendly, it’s very much easy to used it, just like the isotropic models and it is advantageous to use HDKR since it produces results that are closer to the measured values.

3.3 Cell temperature model and Solar PV output prediction

The efficiency, η, of a photovoltaic (PV) array is a function of cell temperature and array irradiation. The study opted for Hove Model illustrated in equation 33, in order to model the cell temperature because it is easy to use, it requires computations at nominal operating cell temperature (NOCT) conditions of which the manufacturers of the PVs already provides. Computation of the cell temperature by this model was now used to predict the electrical output of the PV array given by equation 33 developed by Hove.

$$\boldsymbol{P_{PV}} = \frac{\eta_{PV}}{\eta_{STC}} \cdot \frac{G_T}{G_{STC}} \cdot \boldsymbol{P_{STC}} \quad \text{………………………………………….. (33)}$$

Where,

$\boldsymbol{\eta_{PV}}$ is the PV efficiency

$\boldsymbol{\eta_{STC}}$ is the PV efficiency measured at standard test conditions (STC)

$\boldsymbol{G_T}$ is the incident solar irradiance on the plane of the PV array

G_{STC} is the incident solar irradiance at standard test conditions

$\boldsymbol{P_{STC}}$ is the rated power output of the PV array measured at STC

3.4 Economic analysis consideration

There are three fundamental classifications of the total costs incurred through the lifetime of the designed PV system. Those are initial costs (IC), operation and maintenance costs (O&M) and replacement costs (RC). IC involve all costs incurred in purchasing the components of the system and installing them while O&M include system components maintenance and the overall fuel costs to be used to run a diesel generator. Finally, RC involve the costs of a number of system parameters to be replaced due to reaching their lifespan before that of the PV array.

The formula stated in equation 30 is thus used to calculate the net present cost (NPC) of each component as the sum of lifecycle discounted costs.

Listed in table 4 are the used economic parameters for evaluating the economic model in this study as already described.

Table 4: Economic parameters used in the model

PV array lifespan	25 years
Battery lifespan	7 years
Inverter lifespan	15 years
DG lifespan	6 years
PV capital cost	0.3 $/W
Battery cost	0.1 $/Wh
Inverter cost	0.1 $/W
DG cost	0.1 $/W
DG maintenance	0.15 of capital cost per annum

Specific fuel consumption	0.35 litre/kWh
Fuel cost	1.1 $/litre
Inverter maintenance	0.05 of capital cost per annum
Electricity price	0.1 $/kWh
Discount rate	10%
Battery maintenance cost	0.05 of capital cost per annum
Installation cost	0.4 of capital cost per annum

3.5 Sizing the system and optimization

The PV array size, battery capacity, diesel generator rated power as well as the employed diesel generator energy dispatch strategy are the fundamental variables that control the energy performance of the system for a considered load and diurnal profile. For system optimization, several objective functions such as a system with high renewable fraction, low greenhouse gas emissions and low energy cost are considered. For this current study, minimizing the cost of energy (low LCOE) was opted for as the main objective study employed for system optimization.

With the employed objective function for the current study, selected combination of components sizes is done with reference to a guarantee that needed energy is delivered at all times in order to archive a desired degree of supply reliability. The combination resulting in the least energy cost is the chosen optimum system. The current study represents the designed system component sizes in dimensionless parameters in order to generalize the sizing curves for all magnitudes of daily loads with the same diurnal profile.

As opposed to Hove and Tazvinga, 2012 [90], where dimensionless parameters $\boldsymbol{A/A_0}$ (where $\boldsymbol{A}$ is the actual installed PV array area [m^2] and $\boldsymbol{A_0}$ is a hypothetical area conceptualized by Hove (2000) as the PV array area required for satisfying a daily electrical load constantly throughout the day) were used to characterize the PV size, the model developed by this study opted for the PV array dimensionless input parameter $\boldsymbol{P/P_0}$ instead as well as the battery size dimensionless parameters $\boldsymbol{B_{cap}/L_{day}}$, where $\boldsymbol{P_0}$ is the daily average power given by equation 34, $\boldsymbol{P}$ is the actual PV array power, B_{cap} is the installed battery capacity and $\boldsymbol{L_{day}}$ is the daily load.

$$\boldsymbol{P_0 = \frac{Daily\ load}{24\ hours}} \quad \ldots\ldots\ldots\ldots\ldots\ldots\ldots\ldots\ldots\ldots\ldots\ldots\ldots\ldots \text{(34)}$$

The use of the $\boldsymbol{P/P_0}$ dimensionless parameters for the PV array in this current study was taken as a further illustration of Hove 2000 model by relating the actual installed PV array area $\boldsymbol{A}$ and the actual PV array power $\boldsymbol{P}$ using the equations 35, 36 and 37.

$$\boldsymbol{P_{pv} = G_T \eta_{pv} A} \quad \text{…………………………} (35)$$

At standard test conditions,

$$\boldsymbol{P_{STC} = G_{STC} \eta_{STC} A} \quad \text{…………………………} (36)$$

Thus, from equation 36, actual installed PV array area can be determined in terms of power as shown in equation 37.

$$\mathbf{A} = \frac{\mathbf{P_{STC}}}{\mathbf{G_{STC}\eta_{STC}}} \quad \text{…………………………………………} (37)$$

Substituting equation 37 into equation 35 yields PV power output independent of the array area, which is the equation illustrated in equation 33. The normalized diesel generator variable is given by $\boldsymbol{Q_{DG}/\bar{L}}$ where $\boldsymbol{\bar{L}}$ is the average daily load illustrated mathematically as in equation 38 and $\boldsymbol{Q_{DG}}$ is the diesel generator rated power output.

$$\bar{\mathbf{L}} = \frac{\mathbf{L_{day}}}{\mathbf{24\ hours}} \quad \text{…………………………………………………} (38)$$

3.6 Energy management

Summation of the power from the PV determined using equation 33, the rated power of the backup diesel generator as well as the stored energy by the batteries at each hour, gives the capacity of the developed hybrid system. The amount of output power of the PV array is the primary supply of the load. The PV output power may be sufficient to supply the demand alone but at times at which there is a deficit, the storage batteries supply the remaining or unmet load. If both the output power from the PV array and the one supplied by the batteries still cannot meet all the load, the backup diesel generator is turned on. If the load still cannot all be met, then there will be some unmet load, which can result in load shading or just a supply of critical loads depending on the system developer’s choice [91].

Magnitude of the load as well as the state of charge of the storage battery determines whether the electrical energy generated by the solar PV array and the diesel generator can be used to supply the total load, charge the battery as well as dumping the excess. The illustrated energy management system flowchart in figure 10 provides systematic energy flow in operation of the system[91].

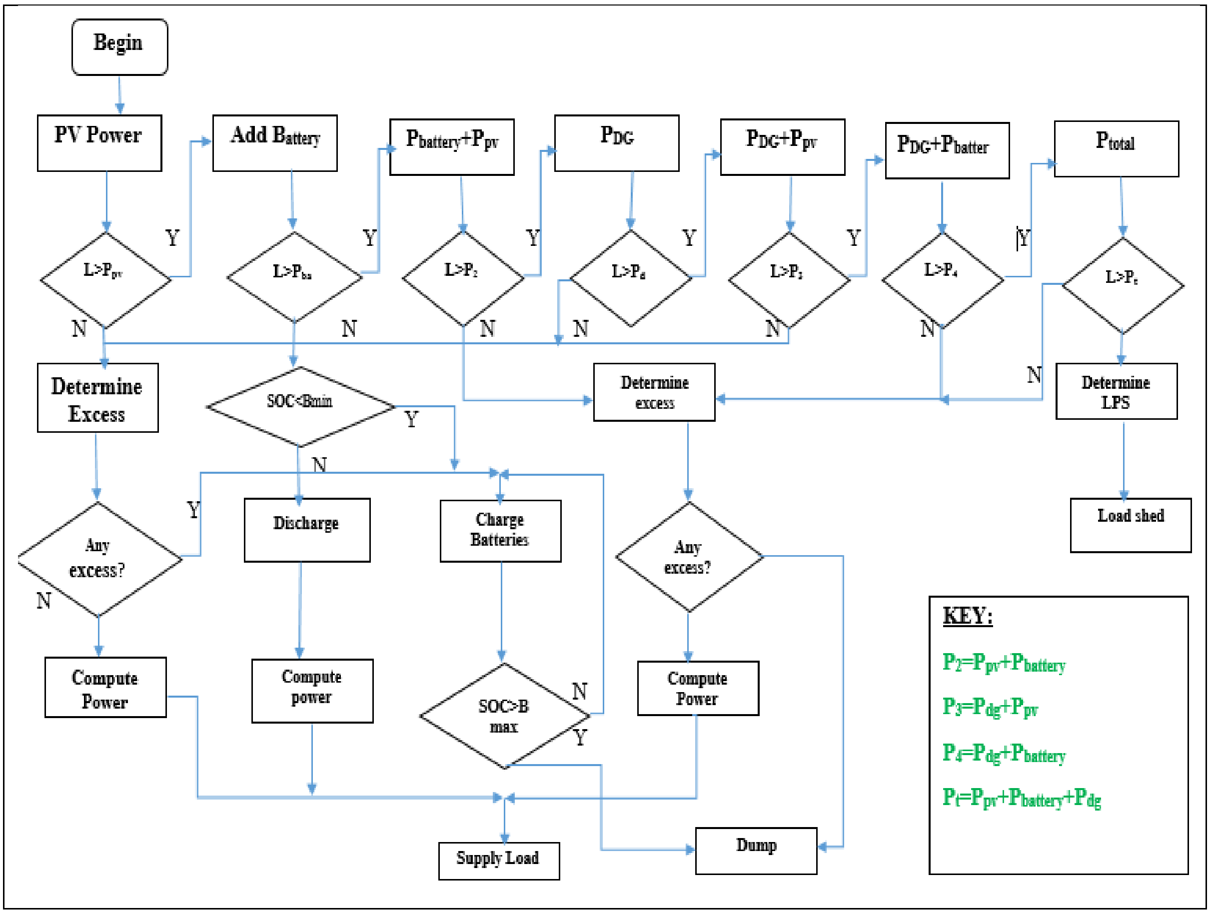

Figure 10: A brief description of the energy management system flowchart

The energy management flowchart illustrated in figure 10 can be explained briefly as follows: The load can be classified differently as it can take any value in the following categories: $L < \eta_{Inv}Q_{PV}$; $\eta_{Inv}Q_{PV} \leq L \leq Q_B + \eta_{Inv}Q_{PV}$; $L > Q_B + \eta_{Inv}Q_{PV}$; where L is the load, Q_{DG} is the diesel generator rated power output, Q_{PV} is the hourly average PV array output, Q_B is the energy supply by the battery and η_{Inv} is the inverter efficiency. As a result, each load category yield a different energy as outlined by Hove et. al [90]. If $L < \eta_{Inv}Q_{PV}$, then PV power is enough to supply the load on its own, with the excess used to charge the batteries provided their state of charge (SOC) is less than the maximum charge of the battery, else the excess is dumped.

If $\eta_{Inv}Q_{PV} < L \leq Q_B + \eta_{Inv}Q_{PV}$, the load is supplied by a combination of both PV array power and the battery bank. All of the PV array output is consumed by the load with the deficit supplied by the batteries. If $L > Q_B + \eta_{Inv}Q_{PV}$, the combine output power from the PV array and the battery is not enough to supply the total load, hence the backup diesel generator is brought in. Since the generator works at its rated power, it will supply the load and if there will be excess, it will combine with the power from the PV array to charge the batteries depending on their state of charge, otherwise it is dumped. If Q_{DG} is not enough to supply the load, the deficit is supplied by PV output power with the excess if any used to charge batteries depending on their SOC.

If the combination of the battery and diesel generator is not enough to supply the load, the deficit is supplied by the batteries provided their state of charge allows that and if not, the system will have to load shed.

3.7 Model Inputs and Outputs

The fundamental three input variables to this developed model are the dimensionless parameters $\boldsymbol{P/P_0}$ (PV array dimensionless input parameter), $\boldsymbol{B_{cap}/L_{day}}$ (the battery size dimensionless parameter) and $\boldsymbol{Q_{DG}/\bar{L}}$ (diesel generator dimensionless variable). The other input variables to the model are as illustrated in table 5.

Table 5: PV array and Battery input parameters to the model

Input parameters	Unit	Values
	PV Array	
Latitude	Degree	Varies in the model depending on the chosen place
Tilt Angle	Degree	Varied in the model to determine the optimal tilt
Azimuth	Degree	180
$\mathbf{P/P_0}$	Dimensionless	Model calculated
Reference efficiency	Percentage (%)	25

Temperature Coefficient		-0.35%
Battery		
$\mathbf{B_{cap}/L_{day}}$	Dimensionless	Model calculated
Battery capacity, B_{cap}	kWh	Model calculated
Minimum state of charge (SOC)	Percentage (%)	20
Maximum depth of discharge (DOD)	Percentage (%)	80
Battery Charging Efficiency, (η_{BATT})	Percentage (%)	95
Battery voltage	Volts (V)	12 V
Diesel Generator		
$\mathbf{Q_{DG}/\bar{L}}$	Dimensionless	Model calculated

The outputs of the model include among others the hourly energy balance of the micro-energy system, photovoltaic array power needed, inverter power and battery energy capacity. The model also output the energy supply reliability, the solar fraction, dumped PV energy and more importantly the Levelized Cost of Energy (LCOE). Table 6 provides summarized outputs table.

Table 6: Outputs to the model

Model Outputs
Annual Global tilted Irradiation PV production
Required PV Array Power
Annual PV Power Output
Annual reliability (partial) Annual load met
Reliability, partial and strict
Solar Fraction
Levelised Cost of Energy (LCOE)
Carbon dioxide (CO_2) emission

Chapter 4

4. Results and discussion

This chapter present the system sizing, modelling, simulation as well as optimization results for the choice of the best solar mini-grid system with reference to the architectural structure combination. Included in the results are the generation from the diesel generator, solar PV array as well as the battery backup, consumed energy, Levelised cost of energy, greenhouse gas emissions and the net present value. Annual system production (comprising of PV production, diesel generator and battery bank) for the case study place, Sehong-hong, is also included in the results.

Comparing traditional and time-step methods of system sizing

System sizing using traditional approach

PV array sizing

Specifications of the chosen panel is illustrated as in table 7:

Table 7: Selected solar panel specifications

Panel Manufacturer	Canadian Solar
Cell type	**Poly-crystalline**
Number of cells	**72 cells**
Maximum power rating STC (Pmax)	**324 watts**
Open circuit voltage (Voc)	**46.2 volts**
Short circuit current (Isc)	**9.79 amps**
Maximum power voltage (Vmp)	**38.1 volts**
Maximum power current (Imp)	**9.2 amps**

Required daily energy from the solar array is determined using equation 33 as follows:

$$E_r = \frac{daily\ average\ energy\ consumption}{product\ of\ components'efficiencies} = \frac{879.23kW}{0.8} = 1099.04\, {}^{kWh}/_{day}$$

Using equation 34, the peak power of the PV is found as:

$$P_p = \frac{E_r}{T_{min}} = \frac{1099.04}{5.5} = 200kW_p$$

The total current needed can be calculated is equation 35 as:

$$I_{DC} = \frac{Peak\ power}{system\ DC\ voltage} = \frac{200000W_p}{48v} = 4166.6A$$

In order to meet the desired voltage and current of the system, modules must be connected in series and parallel using equations 36 and 37 respectively as follows:

$$N_p = \frac{whole\ module\ current}{module\ rated\ current} = \frac{4166.6}{9.2} = 452.9 \cong 453\ panels$$

$$N_s = \frac{system\ DC\ voltage}{module\ rated\ voltage} = \frac{48}{48} = 1$$

Therefore, the total number of modules $N_m = 453x1 = 453\ panels$ in parallel**.**

<u>Battery sizing</u>

Specifications of the chosen battery is illustrated as in table 8:

Table 8: Selected battery specifications

Manufacturer	**Edison**
Model	**LFP700Ah**
Battery	**48 V**
Minimum SOC	**20%**
Nominal Capacity	**370 Ah**
Efficiency	**95%**

Total average energy use is 879.23 kWh. Days of autonomy are selected with reference to [85]. Thus, amount of energy storage required is calculated using equation 38 as follows:

$$E_{rough} = ExD = 879.23x3 = 2637.6kWh$$

For energy safety, $E_{safe} = \frac{E_{rough}}{MDOD} = \frac{2637.6kWh}{0.8} = 3297.11kWh$

Therefore, the needed battery bank capacity is evaluated using equation 40 as follows:

$$C = \frac{E_{safe}}{V_b} = \frac{3297.11kWh}{48v} = 68689.8\ Ah$$

The total number of batteries needed is obtained using equation 41 as follows:

$$N_{batteries} = \frac{C}{C_b} = \frac{68689.8Ah}{370Ah} = 185.6 \cong 186 \; batteries$$

Inverter sizing

AC appliances total power is 879.23 kW

Inverter capacity (25 % bigger than AC appliances total power) is 1099 kW

System sizing using the model (time-step approach)

The actual system parameters such as PV array power required, battery capacity, inverter chargers, etc. are determined by the model using the dimensionless parameters P/P_0, $Q_{DG}/\bar{L}$ and B_{cap}/L_{day}. Depending on the system configuration under analysis, the model predicts amount of different system components needed. Figure 11 illustrate a system configuration (PV and battery backup) which has been analyzed and yielded system components as shown. The system components show among others the total number of PV panels needed, number of PV panels strings, number of string per inverter and the PV array power. The rated battery capacity, number of battery strings as well as the total number of batteries are also shown. PV inerter components and inverter chargers.

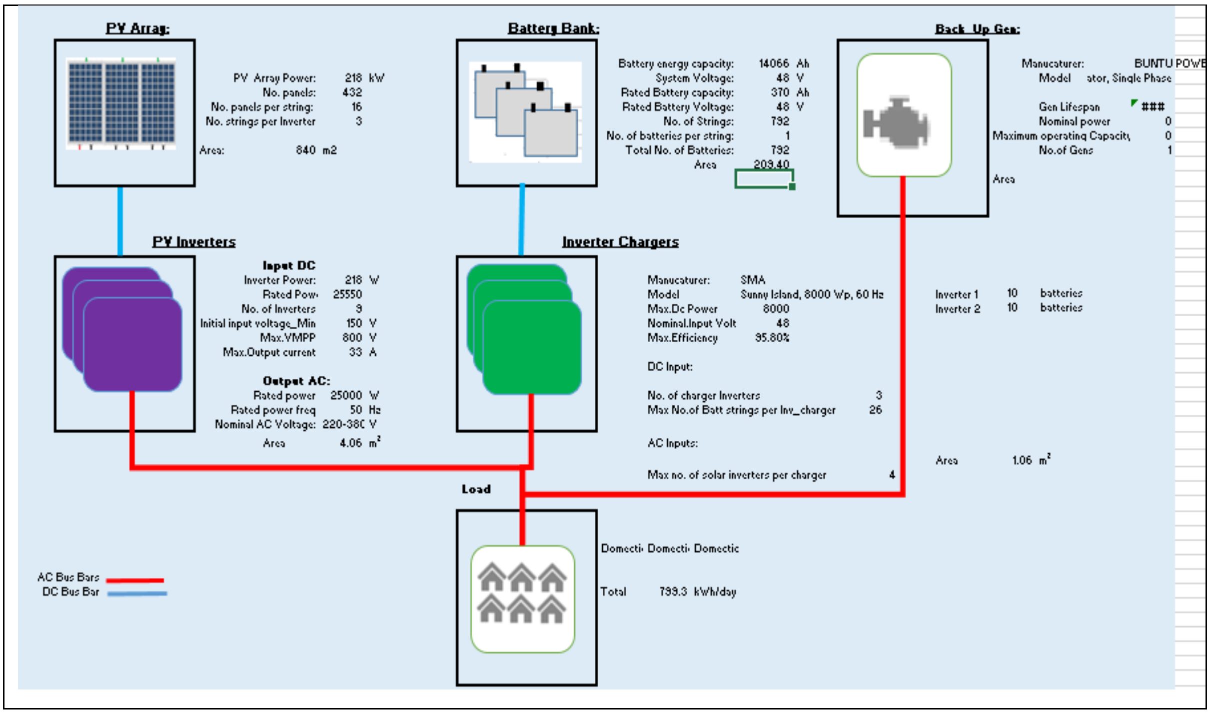

Figure 11: Analyzed system configuration predicting different system components

Now, comparing the sizing results illustrated under traditional approach and the model (using time-step approach), the following observations were figured:

The battery bank capacity needed under the traditional approach is found to be $68689.8\ Ah$ whereas under time-step approach is $14066\ Ah$, which is approximately 5 times less than that in traditional approach. Thus, it is evident from this that the traditional sizing of the storage batteries required is 5 times larger than sized storage under time-step approach. This in turn reflects 5 times the cost associated with the battery sizing, a significant disadvantage of this traditional approach of sizing. Sizing of the Array from the two methods provide approximately the same required number of panels.

Inverter sizing (time-step)

From equation 34, the peak power was found to be $200\ kW_p$. For safety purposes, 25% of the peak power is chosen, giving the total power of $250\ kWp$. This is the inverter size need under using a time-step method as opposed to $1099\ kW$ inverter determined by traditional method. The time-step approach method shows that the required inverter in not necessarily the same size as the total AC appliances total power since it is not possible for all AC appliances to be ON at the same time with reference to the time of use incurred in this method when developing the load profile. This approach has a significant implication on costs since the needed inverter will be smaller as opposed to the one determined under traditional approach. Therefore, the time-step approach is found to be the cost-effective approach of sizing the solar photovoltaic systems. The comparisons were done for a PV and battery system and time-step approach being the determined best economical method for system sizing will be deployed in all other system configurations.

Comparisons of different architectural configurations (at 100% reliability):

Three solar configurations namely system 1 (comprising PV and diesel generator), system 2 (PV and battery backup) and system 3 (PV, battery bank and diesel generator backup) were investigated and classified according to the cost of energy. Selection of the best system configuration was investigated initially by comparing the cost of energy (LCOE) for all the systems when each system provides needed energy 100% of the time (100% Reliability). In all the three system configurations, the diesel dispatch strategy employed is charge cycling control, where by the generator runs at its rated power to supply the load as well as charging the battery bank with the excess.

The best three systems (1, 2 and 3) architectures are summarized as shown in table 7 with baseline (diesel generator only) included for comparison purposes:

Table 9: Summarized solar PV best system architectural configurations

Capacity	**Baseline (Diesel-generator only)**	**System 1 (PV+ Diesel generator)**	**System 2 (PV + Battery)**	**System 3 (PV + Battery + Diesel generator)**
	AC Primary Load (879.2 kWh/day; Sehong-hong place)			
P/P_0	-	23.5	15	11.2
$Q_{DG}/\bar{L}$	2.2	1.22	-	1.22
B_{cap}/L_{day}	-	-	1.8	0.81
PV inverters *(kW)*	-	384	264	147
Number of Inverter chargers	-	8	3	2
LCOE *(USD/kWh)*	0.78	0.70	0.68	0.62
Solar fraction	-	48.2%	100%	82.95%
Reliability	100%	100%	100%	100%
Carbon Emission *(kg/year)*	991,964.95	372364.26	0	53622.56
NPV *(USD)*	2,174,298.00	919,289.12	870,796.08	670,695.69
Dispatch strategy	24 hours/day	Cycle charging		Cycle charging

Summarized simulation results illustrated in table 7 show that the cost of buying energy is lowest in system 3 (0.62 *USD/kWh*), with the solar fraction of 83%. Emitted carbon is 53 623 *kg/year*. Thus, for an objective function of least cost of energy, system 3 will be selected. Likewise, system 2 is the second best based on LCOE (0.68 *USD/kWh*) though it becomes best when comparison is made based on carbon emission since it emits 0 *kg/ year* as well as bigger solar fraction (100%). Lastly, system 1 is the costliest of the three systems (0.7 *USD/kWh*) with the smallest solar fraction (48.2%) and largest carbon emission (372 364.3 *kg/ year*).

For a chosen case study site, Sehong-hong, with daily load of 879.2 kW, the chosen best system (system 3) with a solar system configuration of PV array ($P/P_0 = 11.2$), battery bank ($B_{cap}/L_{day} = 0.8$) and diesel generator ($Q_{DG}/\bar{L} = 1.22$), offers the lowest solar PV (147 kW), storage (17 strings), inverter (147 kW) and LCOE (0.62 USD/ kWh) compared to the systems 1 and 2. The dispatch strategy chosen is the cycle charging for all the systems. System 1 in particular, has the largest solar PV array size ($P/P_0 = 23.5$) so that it can be able to supply the whole load during sunshine hours since it doesn't have a storing system.

System 2 doesn't have the diesel generator backup, hence the bigger storage ($B_{cap}/L_{day} = 2.21$). The solar PV capacity as opposed to system 1 is reduced though it constitutes bigger storage, enough to store more energy to serve the load at times when PV doesn't produce enough to supply the load or produces nothing at all. Reduced solar PV capacity ($P/P_0 = 11.2$) in system 3 as well as battery bank ($B_{cap}/L_{day} = 1.8$) is brought by the fact that the system comprises PV array, battery bank as well as diesel generator backup ($Q_{DG}/\bar{L} = 1.22$). Therefore, whenever PV array doesn't produce enough to serve the load, the deficit is supplied by the battery. If the deficit is still there, the diesel generator will start and load will be supplied by the generator with excess power from the generator combined with power from the PV combined and used to charge the batteries.

In this study, the objective function is the Levelised Cost of Energy at a specified reliability. Therefore, system 3 is chosen to as the best solar system configuration for Lesotho capable of providing needed energy at the lowest costs. Comparing system 3 and a diesel generator only configuration shows that 83% of the costs are saved in system 3 as opposed to a diesel only. With now best system chosen, optimization of the chosen system was performed with dimensionless sizes of battery and PV array required to achieve a desired level of reliability with a minimum Levelized cost of energy are illustrated in table 8.

Table 10: Design space for selection of optimum designs meeting specific levels of reliability

Supply Reliability	**LCOE (USD/kw)**	P/P_0	B_{cap}/L_{day}
99%	0.3	3.9	0.292
98%	0.27	3.5	0.3
97%	0.26	3.4	0.3

96%	0.25	3.2	0.31
95%	0.24	3	0.33
94%	0.225	2.89	0.33
93%	0.22	2.8	0.34
92%	0.212	2.77	0.34
91%	0.21	2.6	0.343
90%	0.20	2.55	0.343

With $Q_{DG}/\bar{L}$ fixed at 1.22, different combinations of P/P_0 and B_{cap}/L_{day} were selected at a defined reliability (from 90% to 100%) and the combination that resulted in the lowest LCOE at a defined reliability as shown in table 10 was selected and plotted as shown in figure 12.

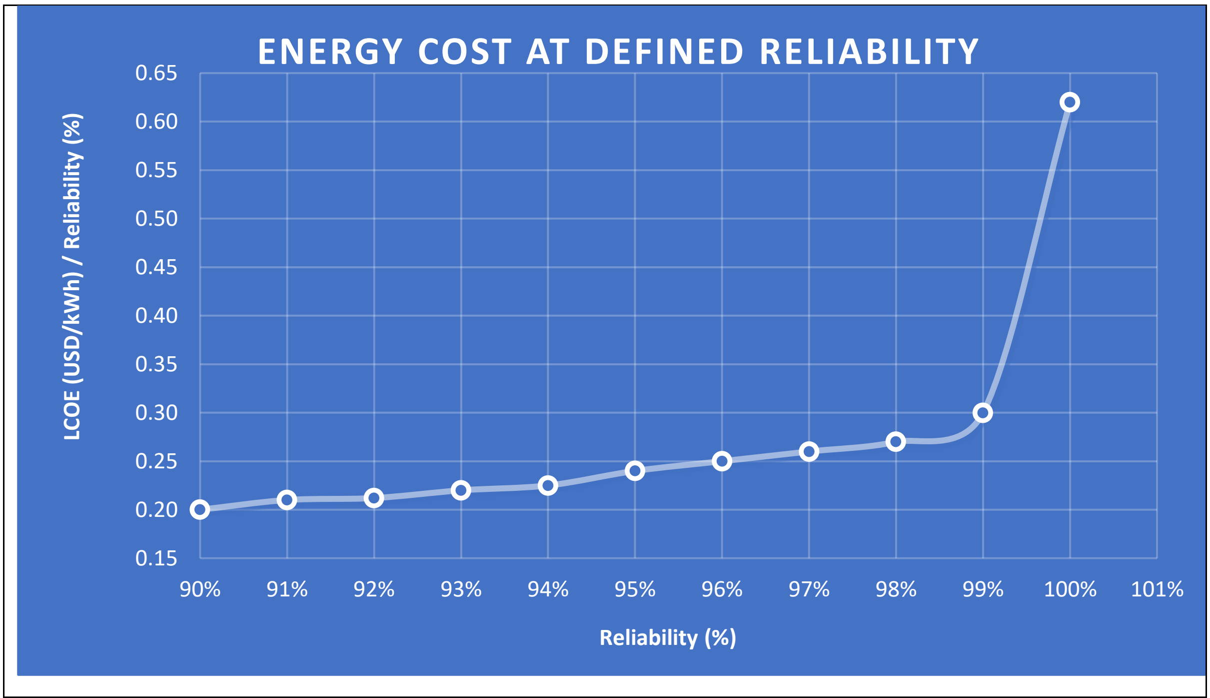

Figure 12: Energy cost at different reliabilities for Sehong-hong

The reliability ranges of 90-100% was chosen with reference to the country's recommended (minimum) 95% reliability of supply for any power supply system. From the optimization performance shown in figure 12, an optimal supply reliability was determined to be 99% (with LCOE of 0.30 *USD/kWh*) using an engineering intuition known as "reliability at the knee of the curve". This is the cost effective point providing much needed benefits (high reliability) from the power system at the least cost. Figure 12 shows that it is uneconomical to design a system at 100% reliability since it approximately doubles the cost of energy with just 1% increase from the cost effective point of 99% reliability. This drastic rise in the energy cost at

100% reliability is brought by the fact that the storage needed to supply much needed energy at every second is too big since consideration of cloudy times of each day need to be considered so that the load will always be met without any failure.

The Levelised Cost of Energy determined by the model (0.30 *USD/kWh*) was compared with the results from the conducted study in Lesotho by One Power for designing a mini-grid for a reference community known as Ha Makebe to perform resource allocation and sizing optimization of energy generation infrastructure based on statistical load estimates. The result of the LCOE determined by this model with found to be in line with the 0.35 *USD/kWh* found for Ha Makebe mini-grid [92] which has the same diurnal profile as Sehong-hong.

Comparison of the annual energy production and consumption, excess energy, unmet load, solar fraction, LCOE and carbon emission for the three systems at 100% supply reliability for Sehong-hong was performed and results shown in table 9.

Table 11: Comparison of the three systems in terms of energy production and consumption

	System 1	System 2	System 3
Total production	**834.866 MWh/year**	**748.054 MWh/year**	**541.138 MWh/year**
➢ **Annual solar PV**	362.214 MWh/year	569.624 MWh/year	412.450 MWh/year
➢ **Backup generator**	472.652 MWh/year	**NOT USED**	19.575 MWh/year
➢ **Battery bank**	**NO USED**	178.430 MWh/year	109.113 MWh/year
AC Primary Load	320.918 MWh/year	320.918 MWh/year	320.918 MWh/year
Annual excess power	513.948 MWh/year	427.136 MWh/year	220. 220 MWh/year
Unmet Load	9.23 MWh/year	20.54 MWh/year	0
Solar fraction	48.20%	100.00%	82.95%
LCOE	0.7 USD/kWh	0.68 USD/kWh	0.62 USD/kWh
Carbon Emission	472364.26 kg/year	0	77354.08 kg/year
Annual reliability (partial)	100.00%	100.00%	100.00%
NPV	919,289.12 USD	870,796.08 USD	670,695.69 USD

As shown in table 9, the total energy production of system 3 (solar PV + Battery bank + Diesel generator) is 541.138 MWh/year comprising of 412.450 MWh/year produced by the photovoltaic array. PV array contributes 76.2% of the total energy produced followed by the 20.2% (109.113 MWh/year) contribution from the battery bank and the remainder being the contribution from the diesel generator backup amounting to 3.6% (19.575 MWh/year) of the total production. The total load (320.918 MWh/year) is met in system 3 leaving an excess of 220. 220 MWh/year and also the system provide the lowest Levelised cost of energy (0.62 USD/kWh) at a partial and strict reliability of 100.00%.

Likewise, system 2 (solar PV + Battery bank) has the total energy production of 748.054 MWh/year which constitutes 76.1% (569.624 MWh/year) produced by the photovoltaic array and 23.9% (178.430 MWh/year) contribution from the battery. There is 20.54 MWh/year of an unmet load in system 2, which is 6.4% of the total AC primary load and an energy excess of 427.136 MWh/year and the system provide the Levelised cost of energy of 0.68 USD/kWh at a strict reliability of 100%. Lastly, system 1 (comprising PV and diesel generator) entails a total energy production of 834.866 MWh/year with 43.3% (362.214 MWh/year) contributed by the PV array and the remaining 56.7% (472.652 MWh/year) contributed by the diesel generator backup. This system has an unmet load of 9.23 MWh/year (which is 1.1% of the total AC primary load) and an energy excess of 513.948 MWh/year. The Levelised cost of energy in system 1 is 0.70 USD/kWh.

Economically system 3 is cheaper with the net present value of 670,695.69 USD, with a 100.00% system reliability of supply. The Levelised cost of energy is lowest for system 3 (0.62 USD/kWh) with a solar fraction of 82.95% and zero annual load unmet. Thus, system 3 is the best architectural configuration with Levelised cost of energy being an objective function. Carbon emission is zero in system 2 since the combination in that system doesn't include a diesel generator, hence 100.00% solar fraction. Therefore, system 2 is the best architectural combination if carbon emission is used as an objective function.

Table 10 illustrates the summarized yearly performance of the three systems as well the Levelised cost of energy for the three systems at 100% supply reliability.

Table 12: Performance comparison for the three system configurations

Systems	LCOE($/kWh)	Solar Fraction (%)	Carbon Emission (kg/MWh)
1	0.70	48.20	472
2	0.68	100	0
3	0.62	82.95	77

Table 10 results show that system 3 (PV + Battery + Generator) offers the best economic option with the LCOE of **0.62 $/kWh** and a second best solar fraction of **82.95%**. The system is also ranked second in terms of carbon emission (**77 kg/MWh**) and from table 8, system 3 meet all the load (zero unmet load) with an excess of **220.220 MWh/year** of electricity.

Chapter 5

5. Conclusions

This study presented the optimized architectural configurations of stand-alone solar mini-grids comprising of the solar PV, battery bank, solar inverters, solar chargers and diesel generator in Lesotho. Using an excel based Microsoft program, integrated modelling, simulation, optimization as well as control methods have been used in this present study to decide on an ideal recommended solar mini-grid best architectural combination in terms of performance as well as the Levelised cost of the system. Simulation results outlined that the best system configuration (solar PV + battery bank + diesel generator) manage to supply all its daily load.

Comparison of the two approaches used for sizing solar PV systems showed that time-step approach is the most cost-effective way of sizing the PV systems. The battery bank capacity needed is approximately 5 times less than that in traditional approach, reflecting 5 times the cost associated with the battery sizing, which is a significant advantage of time-step approach of sizing. Sizing of the Array from the two methods provide approximately the same required number of panels. The time-step approach method shows that the required inverter in not necessarily the same size as the total AC appliances total power since it is not possible for all AC appliances to be ON at the same time with reference to the time of use incurred in this method when developing the load profile. This approach has a significant implication on costs since the needed inverter will be smaller as opposed to the one determined under traditional approach. Therefore, the time-step approach is found to be the cost-effective approach of sizing the solar photovoltaic systems. The comparisons were done for a PV and battery system and time-step approach being the determined best economical method for system sizing will be deployed in all other system configurations.

The best chosen system (system 3) architecture investigated in Sehong-hong area having a daily load of *879.2 kW* required solar PV capacity ($P/P_0 = 11.2$, battery bank ($B_{cap}/L_{day} = 0.81$) as well as diesel generator backup ($Q_{DG}/\bar{L} = 1.22$) to attain 100% supply reliability with the cost of energy found to be 0.62 *USD/kWh*. To generalize the study findings to all parts of the country involves scaling up or down the dimensionless parameters P/P_0, B_{cap}/L_{day} and $Q_{DG}/\bar{L}$ depending on the load of that particular area.

Optimization of the chosen system determined the cost effective supply reliability of 99% (with LCOE of 0.30 *USD/kWh*, $P/P_0 = 3.9$ and $B_{cap}/L_{day} = 0.292$). This reliability was found to provide much needed benefits (high reliability) from the power system at the least cost. The 100% supply reliability used when the three systems were compared so as to determine the best system with reference to the lowest LCOE was found to be uneconomical since it doubles the cost of energy (0.62 *USD/kWh*) with just 1% increase from the cost effective point of 99% reliability. The chosen diesel generator dispatch strategy in this study is charge cycling.

The Levelised Cost of Energy determined by the model (0.30 *USD/kWh*) was compared with the results from the conducted study in Lesotho by One Power for designing a mini-grid for a reference community known as Ha Makebe to perform resource allocation and sizing optimization of energy generation infrastructure based on statistical load estimates. The result of the LCOE determined by this model with found to be in line with the 0.35 *USD/kWh* found for Ha Makebe mini-grid which has the same diurnal profile as Sehong-hong.

For further research, the use of ground measured solar radiation data is highly recommended for proper results comparisons. The model does not compare different diesel generator dispatch strategies which influence optimal-system component sizing and operational parameters, hence the model should be improved to cater for that as a further research. Also the developed model itself do not determine the battery life for sizing and economic analysis of storage systems for any architectural configuration with storage.

With regard to stated conclusions, the following recommendations were made:

- With the abundance of solar radiation in Lesotho, PV mini-grids have a considerable market either in remote and peri-urban areas. Policies implementations should be effected by the government to meet this market demand and promotes mini-grids deployment and address operational problems.
- Institutions of higher learning that offer training in renewable energy technologies should be resourced and encouraged to train local experts on the design installation, operations and maintenance of PV mini-grid systems.

References

[1] P. Nema, R. K. Nema, and S. Rangnekar, "A current and future state of art development of hybrid energy system using wind and PV-solar: A review," *Renew. Sustain. Energy Rev.*, vol. 13, no. 8, pp. 2096–2103, Oct. 2009, doi: 10.1016/j.rser.2008.10.006.

[2] A. Kumar, P. Mohanty, D. Palit, and A. Chaurey, "Approach for standardization of off-grid electrification projects," *Renew. Sustain. Energy Rev.*, vol. 13, no. 8, pp. 1946–1956, Oct. 2009, doi: 10.1016/j.rser.2009.03.008.

[3] "Medium-Term Renewable Energy Market Report 2015," *Renew. ENERGY*, p. 270, 2015.

[4] M. Franz, N. Peterschmidt, M. Rohrer, and B. Kondev, "MinigridPolicyToolkit_Sep2014_EN.pdf." https://www.ren21.net/Portals/0/documents/Resources/MGT/MinigridPolicyToolkit_Sep2014_EN.pdf (accessed Oct. 21, 2019).

[5] O. Publishing and I. E. Agency, *World Energy Outlook 2010.* Paris: Organisation for Economic Co-operation and Development, 2010.

[6] World Bank, *The World Bank Annual Report 2008: Year In Review*. The World Bank, 2008.

[7] E. Boateng, "The potential socio-economic and environmental impacts of solar PV mini-grid deployment on local communities: A case study of rural island communities on the Volta Lake, Ghana," University of Jyväskylä School of Business and Economics, Finland, 2016.

[8] B. Tenenbaum, C. Greacen, and D. Vaghela, "MINI GRIDS AND THE ARRIVAL OF THE MAIN GRID: LESSONS FROM CAMBODIA, SRI LANKA, AND INDONESIA," Energy Sector Management Assistance Program (ESMAP), Washington, DC: World Bank, Technical Report, 2018.

[9] International Energy Agency, Ed., *World energy outlook 2011*. Paris: OECD, 2011.

[10] C. Catita, P. Redweik, J. Pereira, and M. C. Brito, "Extending solar potential analysis in buildings to vertical facades," *Comput. Geosci.*, vol. 66, pp. 1–12, May 2014, doi: 10.1016/j.cageo.2014.01.002.

[11] Department of Energy (DoE), "FORMULATION OF THE LESOTHO ELECTRICATION MASTER PLAN," Ministry of Energy and Meteorology-Lesotho, Maseru, Lesotho, Off-Grid Master Plan Report (Draft), Jun. 2018.

[12] Department of Energy (DoE), "Scaling-up-renewable-energy-for-low-income-countries-srep-lesotho-investment-plan," Ministry of Energy and Meteorology-Lesotho, Maseru, Lesotho, Nov. 2017.

[13] United Nations Development Programme (UNDP), "Development of Cornerstone Public Policies and Institutional Capacities to accelerate Sustainable Energy for All (SE4All) Progress.," Ministry of Energy and Meteorology (MEM)-Lesotho, Maseru, Lesotho, 2013.
[14] "Solar resource maps of Lesotho." https://solargis.com/maps-and-gis-data/download/lesotho (accessed Nov. 08, 2019).
[15] B. Lohani *et al.*, "INTERNATIONAL ORGANISATIONS," p. 216.
[16] S. Bhattacharyya, "Rural Electrification Through Decentralised Off-grid Systems in Developing Countries," 2013. http://libgen.is/book/index.php?md5=29FF50EF6347CBE950ABD9FB5985A388 (accessed Oct. 21, 2019).
[17] S. Bhattacharyya, "Mini-Grids for the Base of the Pyramid Market: A Critical Review," *Energies*, vol. 11, no. 4, p. 813, Apr. 2018, doi: 10.3390/en11040813.
[18] "An Introduction to Grid-Tied Solar PV Systems," *Cenergy MaxPower*, Apr. 25, 2014. http://www.cenergymaxpower.com/introduction-grid-tied-solar-pv-systems/ (accessed Nov. 12, 2019).
[19] "Information on Solar Photovoltaic Stand-alone, Grid connected & Hybrid Systems." http://www.synergyenviron.com/resources/solar-photovoltaic-systems (accessed Nov. 12, 2019).
[20] EEP, "Opportunities and challenges in the mini-grid sector in Africa," EEP Africa, South Africa, First, 2018.
[21] C. Le Gal, A. Wiese, and P. Freunscht, "Assessment Tool For The Hybridisation Of Minigrids – Case Study In Niger," *Energy Procedia*, vol. 155, pp. 280–285, Nov. 2018, doi: 10.1016/j.egypro.2018.11.050.
[22] D. Palit, K. Sarangi, and Global Network on Energy for Sustainable Development, *Renewable energy-based rural electrification: the mini-grid experience from India*. Copenhagen: Global Network on Energy for Sustainable Development, 2014.
[23] R. K. Viral, T. Bahar, and M. Bansal, "MINI GRID DEVELOPMENT FOR RURAL ELECTRIFICATION IN REMOTE INDIA," vol. 3, no. 3, p. 6, 2013.
[24] T. Day, "The role of renewable energy mini-grids in Kenya's electricity sector," p. 49, 2019.
[25] C. RUUD, "AN ANALYSIS OF THE VIABILITY OF SOLAR PV MINI-GRIDS IN TANZANIA," NORWEGIAN UNIVERSITY OF LIFE SCIENCES, NORWAY, 2013.
[26] D. C. Wekesa and M. N. S. Walkade, "PROJECT REPORT SUBMITTED IN PARTIAL FULFILMENT OF THE REQUIREMENT FOR THE AWARD OF BACHELOR OF SCIENCE DEGREE IN ELECTRICAL AND ELECTRONIC ENGINEERING, UNIVERSITY OF NAIROBI.," p. 64.
[27] Deena, "Rethinking Silicon Valley: The I-V Curve," *Rethinking Silicon Valley*, Feb. 25, 2016. http://deenadoesscience.blogspot.com/2016/02/the-i-v-curve.html (accessed Jan. 22, 2020).
[28] G. Arora, N. Aggarwal, D. Sen, and P. Singh, "Design of Solar Power Inverter," vol. 2, no. 1, p. 5, 2015.
[29] A. Jossen, J. Garche, and D. U. Sauer, "Operation conditions of batteries in PV applications," *Sol. Energy*, vol. 76, no. 6, pp. 759–769, 2004, doi: 10.1016/j.solener.2003.12.013.
[30] P. Manimekalai, R. Harikumar, and S. Raghavan, "An Overview of Batteries for Photovoltaic (PV) Systems," *Int. J. Comput. Appl.*, vol. 82, no. 12, pp. 28–32, Nov. 2013, doi: 10.5120/14170-2299.
[31] D. P. Kaundinya, P. Balachandra, and N. H. Ravindranath, "Grid-connected versus stand-alone energy systems for decentralized power—A review of literature," *Renew. Sustain. Energy Rev.*, vol. 13, no. 8, pp. 2041–2050, Oct. 2009, doi: 10.1016/j.rser.2009.02.002.
[32] D. Palit, G. K. Sarangi, and P. R. Krithika, "Energising Rural India Using Distributed Generation: The Case of Solar Mini-Grids in Chhattisgarh State, India," in *Mini-Grids for Rural Electrification of Developing Countries*, S. C. Bhattacharyya and D. Palit, Eds. Cham: Springer International Publishing, 2014, pp. 313–342.

[33] K. Ulsrud, T. Winther, D. Palit, H. Rohracher, and J. Sandgren, “The Solar Transitions research on solar mini-grids in India: Learning from local cases of innovative socio-technical systems,” *Energy Sustain. Dev.*, vol. 15, no. 3, pp. 293–303, Sep. 2011, doi: 10.1016/j.esd.2011.06.004.

[34] D. Palit, “Solar energy programs for rural electrification: Experiences and lessons from South Asia,” *Energy Sustain. Dev.*, vol. 17, no. 3, pp. 270–279, Jun. 2013, doi: 10.1016/j.esd.2013.01.002.

[35] P. Mohanty and T. Muneer, “Smart Design of Stand-Alone Solar PV System for Off Grid Electrification Projects,” in *Mini-Grids for Rural Electrification of Developing Countries*, S. C. Bhattacharyya and D. Palit, Eds. Cham: Springer International Publishing, 2014, pp. 63–93.

[36] “African Solar Investment and Industry Continues to Grow but Falls Far Short of What’s Needed.” https://solarmagazine.com/african-solar-investment-industry-growing-but-far-short-whats-needed/ (accessed Nov. 12, 2019).

[37] B. Bala and S. A. Siddique, “Optimal design of a PV-diesel hybrid system for electrification of an isolated island—Sandwip in Bangladesh using genetic algorithm,” *Energy Sustain. Dev.*, vol. 13, no. 3, pp. 137–142, Sep. 2009, doi: 10.1016/j.esd.2009.07.002.

[38] “CivicSolar | CivicSolar provides industry-leading service and technology to solar contractors.” https://www.civicsolar.com/ (accessed Oct. 21, 2019).

[39] J. A. Duffie and W. A. Beckman, “Solar Engineering of Thermal Processes,” vol. Fourth Edition, p. 928, Oct. 2005.

[40] A. Q. Jakhrani, S. R. Samo, A. R. H. Rigit, and S. A. Kamboh, “Selection of Models for Calculation of Incident Solar Radiation on Tilted Surfaces,” p. 10, 2013.

[41] M. S. Okundamiya and A. N. Nzeako, “Empirical Model for Estimating Global Solar Radiation on Horizontal Surfaces for Selected Cities in the Six Geopolitical Zones in Nigeria,” *J. Control Sci. Eng.*, vol. 2011, pp. 1–7, 2011, doi: 10.1155/2011/356405.

[42] C. K. Pandey and A. K. Katiyar, “A note on diffuse solar radiation on a tilted surface,” *Energy*, vol. 34, no. 11, pp. 1764–1769, Nov. 2009, doi: 10.1016/j.energy.2009.07.006.

[43] A. Q. Jakhrani, A. K. Othman, A. R. H. Rigit, and S. R. Samo, “Comparison of Solar Photovoltaic Module Temperature Models,” p. 8, 2011.

[44] World Congress on Engineering, International Conference of Manufacturing Engineering and Engineering Management, and International Conference of Mechanical Engineering, *World Congress on Engineering: WCE 2018: 4-6 July 2018, Imperial College London, London U.K. volume 2: ...* Hong Kong: Newswood Limited, IAENG (International Association of Engineers), 2018.

[45] D. Yang, “Solar radiation on inclined surfaces: Corrections and benchmarks,” *Sol. Energy*, vol. 136, pp. 288–302, Oct. 2016, doi: 10.1016/j.solener.2016.06.062.

[46] Gh. A. Kamali, I. Moradi, and A. Khalili, “Estimating solar radiation on tilted surfaces with various orientations: a study case in Karaj (Iran),” *Theor. Appl. Climatol.*, vol. 84, no. 4, pp. 235–241, Mar. 2006, doi: 10.1007/s00704-005-0171-y.

[47] P. G. Loutzenhiser, H. Manz, C. Felsmann, P. A. Strachan, T. Frank, and G. M. Maxwell, “Empirical validation of models to compute solar irradiance on inclined surfaces for building energy simulation,” *Sol. Energy*, vol. 81, no. 2, pp. 254–267, Feb. 2007, doi: 10.1016/j.solener.2006.03.009.

[48] A. Q. Jakhrani, A.-K. Othman, A. R. H. Rigit, S. R. Samo, and S. A. Kamboh, “Estimation of Incident Solar Radiation on Tilted Surface by Different Empirical Models,” vol. 2, no. 12, p. 6, 2012.

[49] A. M. Noorian, I. Moradi, and G. A. Kamali, “Evaluation of 12 models to estimate hourly diffuse irradiation on inclined surfaces,” *Renew. Energy*, p. 7, 2008.

[50] E. G. Evseev and A. I. Kudish, “The assessment of different models to predict the global solar radiation on a surface tilted to the south,” *Sol. Energy*, vol. 83, no. 3, pp. 377–388, Mar. 2009, doi: 10.1016/j.solener.2008.08.010.

[51] T. M. Klucher, “Evaluation of models to predict insolation on tilted surfaces,” *Sol. Energy*, vol. 23, no. 2, pp. 111–114, 1979, doi: 10.1016/0038-092X(79)90110-5.

[52] M. David, P. Lauret, and J. Boland, “Evaluating tilted plane models for solar radiation using comprehensive testing procedures, at a southern hemisphere location,” *Renew. Energy*, vol. 51, pp. 124–131, Mar. 2013, doi: 10.1016/j.renene.2012.08.074.

[53] K. K. Gopinathan, “Solar radiation on variously oriented sloping surfaces,” *Sol. Energy*, vol. 47, no. 3, pp. 173–179, 1991, doi: 10.1016/0038-092X(91)90076-9.

[54] K. N. Shukla, S. Rangnekar, and K. Sudhakar, “Comparative study of isotropic and anisotropic sky models to estimate solar radiation incident on tilted surface: A case study for Bhopal, India,” *Energy Rep.*, vol. 1, pp. 96–103, Nov. 2015, doi: 10.1016/j.egyr.2015.03.003.

[55] R. Mubarak, M. Hofmann, S. Riechelmann, and G. Seckmeyer, “Comparison of Modelled and Measured Tilted Solar Irradiance for Photovoltaic Applications,” *Energies*, vol. 10, no. 11, p. 1688, Oct. 2017, doi: 10.3390/en10111688.

[56] H.-J. Lee, S.-Y. Kim, and C.-Y. Yun, “Comparison of Solar Radiation Models to Estimate Direct Normal Irradiance for Korea,” p. 12, 2017.

[57] C. Demain, “Evaluation of different models to estimate the global solar radiation on inclined surfaces,” *Renew. Energy*, p. 12, 2013.

[58] M. Despotovic, “Evaluation of empirical models for predicting monthly mean horizontal diffuse solar radiation,” *Renew. Sustain. Energy Rev.*, p. 15, 2016.

[59] A. Q. Jakhrani, S. R. Samo, S. A. Kamboh, J. Labadin, and A. R. H. Rigit, “An Improved Mathematical Model for Computing Power Output of Solar Photovoltaic Modules,” *Int. J. Photoenergy*, vol. 2014, pp. 1–9, 2014, doi: 10.1155/2014/346704.

[60] A. R. Jatoi, S. R. Samo, and A. Q. Jakhrani, “An Improved Empirical Model for Estimation of Temperature Effect on Performance of Photovoltaic Modules,” *Int. J. Photoenergy*, vol. 2019, pp. 1–16, Jul. 2019, doi: 10.1155/2019/1681353.

[61] A. Rouholamini, H. Pourgharibshahi, R. Fadaeinedjad, and M. Abdolzadeh, “Temperature of a photovoltaic module under the influence of different environmental conditions – experimental investigation,” *Int. J. Ambient Energy*, vol. 37, no. 3, pp. 266–272, May 2016, doi: 10.1080/01430750.2014.952842.

[62] E. Skoplaki, A. G. Boudouvis, and J. A. Palyvos, “A simple correlation for the operating temperature of photovoltaic modules of arbitrary mounting,” *Sol. Energy Mater. Sol. Cells*, vol. 92, no. 11, pp. 1393–1402, Nov. 2008, doi: 10.1016/j.solmat.2008.05.016.

[63] E. Skoplaki and J. A. Palyvos, “On the temperature dependence of photovoltaic module electrical performance: A review of efficiency/power correlations,” *Sol. Energy*, vol. 83, no. 5, pp. 614–624, May 2009, doi: 10.1016/j.solener.2008.10.008.

[64] P. Trinuruk, C. Sorapipatana, and D. Chenvidhya, “Estimating operating cell temperature of BIPV modules in Thailand,” *Renew. Energy*, vol. 34, no. 11, pp. 2515–2523, Nov. 2009, doi: 10.1016/j.renene.2009.02.027.

[65] M. C. Alonso García and J. L. Balenzategui, “Estimation of photovoltaic module yearly temperature and performance based on Nominal Operation Cell Temperature calculations,” *Renew. Energy*, vol. 29, no. 12, pp. 1997–2010, Oct. 2004, doi: 10.1016/j.renene.2004.03.010.

[66] T. Nordmann and L. Clavadetscher, “UNDERSTANDING TEMPERATURE EFFECTS ON PV SYSTEM PERFORMANCE,” p. 4, May 2003.

[67] R. Chenni, M. Makhlouf, T. Kerbache, and A. Bouzid, “A detailed modeling method for photovoltaic cells,” *Energy*, vol. 32, no. 9, pp. 1724–1730, Sep. 2007, doi: 10.1016/j.energy.2006.12.006.

[68] H. A. Rahman, K. M. Nor, M. Y. Hassan, and M. S. Majid, “Empirical Models for the Correlation of Global Solar Radiation Under Malaysia Environment,” p. 8.

[69] M. Almaktar, H. A. Rahman, M. Y. Hassan, and S. Rahman, “Climate-based empirical model for PV module temperature estimation in tropical environment,” *Appl. Sol. Energy*, vol. 49, no. 4, pp. 192–201, Oct. 2013, doi: 10.3103/S0003701X13040026.

[70] T. Hove, “A method for predicting long-term average performance of photovoltaic systems,” *Renew. Energy*, vol. 21, no. 2, pp. 207–229, Oct. 2000, doi: 10.1016/S0960-1481(99)00131-7.
[71] A. M. Muzathik, “Photovoltaic Modules Operating Temperature Estimation Using a Simple Correlation,” *Int. J. Energy Eng.*, vol. 4, p. 8, 2014.
[72] A. Ponniran, N. A. Mamat, and A. Joret, “Electricity Profile Study for Domestic and Commercial Sectors,” 2012.
[73] T. Gönen, *Electric power transmission system engineering analysis and design*, 2. ed. Boca Raton, Fla.: CRC Press, 2009.
[74] G. Kourtis, I. Hadjipaschalis, and A. Poullikkas, “An overview of load demand and price forecasting methodologies,” p. 29.
[75] M. P. Blimpo and M. Cosgrove-Davies, “Electricity Access in Sub-Saharan Africa,” p. 167.
[76] M. Grimm, L. Lenz, J. Peters, and M. Sievert, “Demand for Off-Grid Solar Electricity: Experimental Evidence from Rwanda,” p. 35, 2016.
[77] A. Gupta, R. P. Saini, and M. P. Sharma, “Modelling of hybrid energy system—Part II: Combined dispatch strategies and solution algorithm,” *Renew. Energy*, vol. 36, no. 2, pp. 466–473, Feb. 2011, doi: 10.1016/j.renene.2009.04.035.
[78] T. S. Ong, “Net Present Value and Payback Period for Building Integrated Photovoltaic Projects in Malaysia,” *Int. J. Acad. Res. Bus. Soc. Sci.*, vol. 3, no. 2, p. 19, 2013.
[79] E. F. Brigham and M. C. Ehrhardt, *Financial management: theory and practice*, 12. ed. Mason, Ohio: South-Western Cengage Learning, 2008.
[80] S. R. Jory, A. Benamraoui, D. R. Boojihawon, and N. O. Madichie, “Net Present Value Analysis and the Wealth Creation Process: A Case Illustration,” p. 15, 2016.
[81] O. Žižlavský, “Net Present Value Approach: Method for Economic Assessment of Innovation Projects,” *Procedia - Soc. Behav. Sci.*, vol. 156, pp. 506–512, Nov. 2014, doi: 10.1016/j.sbspro.2014.11.230.
[82] M. EL-Shimy, “Analysis of Levelized Cost of Energy (LCOE) and grid parity for utility-scale photovoltaic generation systems,” 2012, doi: 10.13140/RG.2.2.10311.29603.
[83] A. Castillo Ramírez, D. Mejía Giraldo, and N. Muñoz Galeano, “Large-scale solar PV LCOE comprehensive breakdown methodology,” *CTF - Cienc. Tecnol. Futuro*, vol. 7, no. 1, pp. 117–136, Jan. 2017, doi: 10.29047/01225383.69.
[84] S.-H. Hwang, M.-K. Kim, and H.-S. Ryu, “Real Levelized Cost of Energy with Indirect Costs and Market Value of Variable Renewables: A Study of the Korean Power Market,” *Energies*, vol. 12, no. 13, p. 2459, Jun. 2019, doi: 10.3390/en12132459.
[85] A. N. Al-Shamani, M. Y. H. Othman, S. Mat, M. H. Ruslan, A. M. Abed, and K. Sopian, “Design & Sizing of Stand-alone Solar Power Systems A house Iraq,” p. 7.
[86] A. A. Alabi, A. U. Adoghe, O. G. Ogunle, and C. O. A. Awosope, “Development and sizing of a grid-connected solar PV power plant for Canaanland community,” *Int. J. Appl. Power Eng. IJAPE*, vol. 8, no. 1, p. 69, Apr. 2019, doi: 10.11591/ijape.v8.i1.pp69-77.
[87] D. F. A. Riza and S. I. H. Gilani, “Standalone Photovoltaic System Sizing using Peak Sun Hour Method and Evaluation by TRNSYS Simulation,” p. 7, 2014.
[88] R. Skunpong and B. Plangklang, “A Practical Method for Quickly PV Sizing,” *Procedia Eng.*, vol. 8, pp. 120–127, 2011, doi: 10.1016/j.proeng.2011.03.022.
[89] P. Mohanty, K. R. Sharma, M. Gujar, M. Kolhe, and A. N. Azmi, “PV System Design for Off-Grid Applications,” in *Solar Photovoltaic System Applications*, P. Mohanty, T. Muneer, and M. Kolhe, Eds. Cham: Springer International Publishing, 2016, pp. 49–83.
[90] T. Hove and H. Tazvinga, “A techno-economic model for optimising component sizing and energy dispatch strategy for PV-diesel-battery hybrid power systems,” *J. Energy South. Afr.*, vol. 23, no. 4, pp. 18–28, Oct. 2017, doi: 10.17159/2413-3051/2012/v23i4a3175.
[91] M. Jamshidi and A. Askarzadeh, “Techno-economic analysis and size optimization of an off-grid hybrid photovoltaic, fuel cell and diesel generator system,” *Sustain. Cities Soc.*, vol. 44, pp. 310–320, Jan. 2019, doi: 10.1016/j.scs.2018.10.021.

[92] P. Cicilio, M. Orosz, A. Mueller, and E. Cotilla-Sanchez, “uGrid: Reliable Minigrid Design and Planning Toolset for Rural Electrification,” *IEEE Access*, vol. 7, pp. 163988–163999, 2019, doi: 10.1109/ACCESS.2019.2952896.